1962

Relaxation phenomena in the electrical double-layer

Daniel Harrison Grantham
Iowa State University

RELAXATION PHENOMENA IN THE ELECTRICAL DOUBLE-LAYER

by

Daniel Harrison Grantham

A Dissertation Submitted to the
Graduate Faculty in Partial Fulfillment of
The Requirements for the Degree of
DOCTOR OF PHILOSOPHY

Major Subject: Physical Chemistry

Approved:

Signature was redacted for privacy.

In Charge of Major Work

Signature was redacted for privacy.

Head of Major Department

Signature was redacted for privacy.

Dean of Graduate College

Iowa State University
Of Science and Technology
Ames, Iowa

1962

TABLE OF CONTENTS

INTRODUCTION

Since Quincke (1) introduced the notion of an electrical double layer at the interface between a metal and an electrolytic solution, an entire field of investigation concerned with the properties of the interfacial region has evolved. On the one hand electrochemists (2) have been concerned with the effect of the double layer on the results of investigations of electrode processes, while on the other, surface chemists (3, 4) have investigated changes in double layer properties resulting from adsorption of both charged and uncharged species in the interfacial region. More recently, semi-conducting materials have been immersed in electrolytic solutions and the properties of the interfaces formed have been investigated (5).

The general picture of the double layer which emerges is one of general overall simplicity with rather complex difficulties arising when one attempts to give a detailed description of the local structure and properties of the interface. In a somewhat graphic fashion, the double layer may be supposed to consist of a layer of charge residing on the metal, a layer of solvent molecules adjacent to the metal surface, and a region in the solution in which the charge distribution differs from that of the bulk of the solution. The solvent layer next to the metal is commonly called the compact part of the double layer and the region of altered charge distribution

in the solution is called the diffuse part. The layer of solvent molecules adjacent to the metal may have interspersed among them positive or negative ions from the solution without a solvent sheath on the side of the ion adjacent to the metal surface. Such ions are said to be specifically adsorbed. Neutral molecules may also adsorb and, if long enough, extend through the compact part of the double layer into the diffuse part. Cations usually are not specifically adsorbed while most anions are to some extent. Such concepts as the distance of closest approach for ions become somewhat ambiguous when specific adsorption occurs or when mixtures of electrolytes are discussed. For example, when a specifically adsorbed anion is larger than the cation plus its solvent sheath one can have the plane of centers of the specifically charged ions further removed from the metal surface than the plane through centers of the nearest ions in the diffuse part of the double layer.

Because of the difficulties associated with discussions of the cases previously mentioned, theoretical treatments of the double layer usually are in terms of ideally polarizable interfaces with specific adsorption absent. A polarizable interface is one across which no charge is transferred when a potential is applied from an external source. One finds that this ideal is most nearly approached when the metal is mercury. Complications due to Faradaic processes can thus be avoided

when comparing experiment with theory.

Since charge can accumulate at the mercury-solution interface, the density of charge and its variation with potential are obviously properties of interest. Gibbs (6) and Lippmann (7) showed the relation between surface charge density and surface free energy. Thus, interfacial tension at mercury-solution interfaces is another property which can be investigated as a function of charge density or, more conveniently, potential. It was very early recognized that the interface could be discussed in terms of its capacitance since charge accumulates at metal and solution sides of the interface in the same fashion as on the plates of a capacitor. Early experiments showed an almost constant capacity of 5 microfarads per $cm.^2$ for a wide variety of electrode materials and electrolytic solutions over a range of potentials. It remained for Frumkin (8) to demonstrate the levelling effect of traces of surface active materials in the solution and to show that the capacitance was extremely sensitive to small quantities of these materials. When rigorous purification of materials preceded measurements, the capacitance showed strong dependence on potential and was many times larger than previously found.

Frumkin (8) applied oscillographic techniques to the measurement of capacity. Since the capacity itself is a function of potential, low amplitude signals are necessary and it

must be recognized that one is measuring here a differential capacitance, C, defined by

$$C = \frac{dQ}{dV} \tag{1}$$

where Q is the charge density, V is the applied potential and $\frac{dQ}{dV}$ is the rate of change of charge density with potential. The integral capacity, K, is defined by

$$K = \frac{Q}{V} \tag{2}$$

and the relationship exists that

$$K = \frac{1}{V} \int_0^V C \, dx \tag{3}$$

Grahame (9) refined the alternating current bridge technique and has published results for a wide variety of systems. His experimental apparatus consisted of a bridge, a signal source and a null detector, all of which were standard electronic components. In the balancing arm of the bridge were placed a decade capacitance set and a decade resistance set in parallel combination. The interface between mercury and the solution of interest was formed inside a closed glass system containing the solution and two additional electrodes. One of these was a reference electrode and one pole of the polarizing potential source was connected to this electrode. Grahame commonly used a normal calomel reference electrode with a liquid-liquid junction. The second additional electrode was a dummy electrode of large area compared to that of the mercury-solution

interface and usually was a hollow platinum sphere or a cylindrical platinum gauze. The electrical connections to the bridge were made to the dummy electrode and to the mercury so that continuity was established between the mercury and the dummy electrode through the solution. It was recognized that a second path for conduction existed in parallel with the mercury-solution-dummy electrode path. This was the dummy electrode-solution-reference electrode-potential source path. Insertion of a large inductance in this path greatly reduced the contribution of this extraneous conduction to the overall admittance of the cell. Grahame investigated several interface configurations and found that a droplet extruded from the end of a fine capillary served his purpose best. The capillary tip was oriented so that the hollow spherical dummy electrode was concentric with the mercury droplet.

Theories of the electrical double layer should account for those properties mentioned previously, namely the surface charge density, the capacitance, and surface tension. The theory most commonly accepted as being descriptive of the properties of the double layer actually applies only to the diffuse part of the double layer. Grahame (10) has presented the theory. It rests on the assumption that the Poisson equation relates the charge density to potential within the diffuse part of the double layer according to

$$\nabla^2 \psi = -4\pi\rho \qquad (4)$$

and that the Boltzmann statistics apply to the charge distribution according to

$$n_i = n_{0i} e^{-z_i \epsilon \phi / KT} \tag{5}$$

where ϕ is potential, ρ is charge density, n is concentration of species under the influence of a field, n_{0i} is the bulk concentration of species i and z_i its valence while $z_i \epsilon$ gives the charge of a single ion of type i. These considerations lead to an expression for the surface charge density in the diffuse double layer as follows

$$Q(\phi) = -11.72 \sqrt{c} \sinh 19.46\phi \tag{6}$$

where c is concentration of the solution under study when the solute is a uni-univalent electrolyte and the temperature is 25°C. This charge density gives the quantity of excess charge in a cylinder of unit cross section extending from a point at which the potential is ϕ to the bulk of the solution where the potential is taken to be zero. If ϕ_0 is taken to be the potential at the plane of closest approach of solvated ions, we have an expression for the charge on the diffuse part of the double layer. This is likewise the total charge on the double layer. Differentiation of Q with respect to ϕ leads to an expression for the capacitance of the diffuse part of the double layer.

$$C = 228.5 \sqrt{c} \cosh 19.46\phi \tag{7}$$

So far the potential has not been exactly defined in terms of an experimental operation. In this derivation, ϕ has been

taken as zero when Q is zero. The potential of the mercury relative to a reference electrode, however, is generally not zero when Q is zero so that experimental results must be referred to the potential of zero charge when comparing with theory. The Lippmann equation (11) gives a convenient criterion for the potential of zero charge. In the absence of surface active materials

$$-d\gamma = Q dV \tag{8}$$

where γ is the surface tension. Thus, when Q is zero

$$\frac{d\gamma}{dV} = 0 \tag{9}$$

and the surface tension exhibits a maximum value. Direct measurement of γ as a function of V using a Lippmann capillary electrometer (12) serves to establish the potential of zero charge or the electrocapillary maximum.

Since the potential drop between the mercury and the solution can be divided into as many parts as seem physically significant, we can regard the potential drop across the diffuse part of the double layer as one natural subdivision of the total drop and that which remains may be taken as occurring across the compact part of the double layer. We can associate a capacitance with each of the potential drops and regard the two as being in series combination. The combination law is

$$\frac{1}{C}_{\text{total}} = \frac{1}{C}_{\text{diffuse}} + \frac{1}{C}_{\text{compact}} \tag{10}$$

or

$$\frac{1}{K}_{\text{total}} = \frac{1}{K}_{\text{diffuse}} + \frac{1}{K}_{\text{total}} \qquad (11)$$

for the differential capacitance and the integral capacitance respectively. It is generally held that the capacitance of the diffuse part of the double layer is given to sufficient accuracy by Equation 7 and the capacitance of the compact part of the double layer can be calculated from Equation 10. Inspection of Equation 7 shows that at moderate concentrations the capacity of the diffuse part of the double layer is large, of the order 228.5 microfarads per cm.^{2} at 1 M near the zero charge potential and even larger at other potentials. It follows that the much smaller values measured for the double layer capacitance must actually arise in the compact part of the double layer for concentrations greater than 10^{-3} M. Even if the calculated capacitance of the diffuse double layer is in error by a factor of two or three, this conclusion is still valid. This means that the character of the curves for double layer capacitance as a function of potential arises almost entirely in the compact part of the double layer for these concentrations.

Theories explaining the properties of the compact part of the double layer are much less satisfactory than the Gouy-Chapman theory outlined for the diffuse double layer. From the magnitude of the capacitance and the known dimensions of water molecules, it appears that the dielectric constant of

water in the compact part of the double layer must be much less than that of bulk water. Values from about four to as high as fifteen (10) have been proposed. The most important contribution to the dielectric constant of water is due to the orientational polarizability. The relatively high fields, about 10^6 volts per centimeter, which must exist in the compact part of the double layer, probably contribute to a reduction of the orientational polarizability through dielectric saturation. Debye (13) has treated this phenomenon for gases and concludes that the effect would not be important below 10^5 volts per centimeter. Additional changes in the dielectric constant for water could be caused by the high pressures exerted on the compact part of the double layer by the ions of the diffuse part of the double layer under the attractive influence of the opposite charges on the mercury and by interactions of the water molecules with the mercury.

Most of these effects have been considered separately and collectively by Grahame (14), Ershler (15), and MacDonald (16) with only limited success. Watts-Tobin has recently added a treatment which gives the proper shape of capacity versus charge curves (17).

Due to the lack of a satisfactory theoretical treatment of the compact part of the double layer and the limited amount of information available from such thermodynamic quantities as surface free energy, charge on the double-layer and the like,

it would seem desirable to attempt structure elucidation or to examine the kinetics of the formation of the double layer. Oscillographic traces showing charging rate have been obtained (18). Grahame (19) investigated the effect of frequency of the alternating current through his bridge on the magnitude of the capacitance at a mercury surface in several solutions. He concluded that pools of mercury in small cups showed a decrease in the capacitance for increasing frequency if the pools were of small surface area, presumably about one square centimeter. Larger pools showed less dependence. In the same investigation small growing mercury droplets were investigated as they were extruded from fine glass capillaries. The results were dependent on the capillary used in the formation of the drop. Blunt capillaries showed a decrease in the capacity as the frequency increased. A change of about fifteen per cent was observed when the frequency changed from 250 cycles per second to 5 kilocycles per second. Finer capillaries showed almost no dependence of the capacity on frequency. In all cases the resistive component of the double layer impedance showed a decrease of about fifty per cent on increasing the frequency from 250 cycles per second to 10 kilocycles per second. In an investigation by Frumkin and Melik-Gaikazyan (20) preliminary to a study of adsorption kinetics, no frequency effect on the capacity is reported. Bockris and Conway (21) reported resistance and capacitance as a function of

frequency for copper electrodes in sulfuric acid near the potential of zero charge. The capacitance decreased by about fifty per cent when the frequency was changed from 10 cycles per second to 2 kilocycles per second. Bockris and Conway took care that shielding effects in the mounting of the copper sphere were minimized or eliminated. Grantham (22) found a decrease in capacity of about fifteen per cent when the frequency of the applied signal was changed from 250 cycles per second to 9.2 kilocycles per second. Measurements were on mercury drops pendant from gold plated platinum spheres. Changes in resistance were in rough agreement with those reported by others.

In view of the general agreement in the reported investigations that the resistance arising in the double layer is frequency dependent and the disagreement on the effect of varying frequency on capacity, these measurements of the double layer impedance as a function of frequency were undertaken.

EXPERIMENTAL

Materials

All aqueous solutions were prepared in water having a conductivity of less than 10^{-6} ohm^{-1} cm^{-1}. The water was distilled once from a Barnstead still equipped with a block tin condenser and again from a similar still with potassium hydroxide and potassium permanganate added to the still pot to oxidize any organic matter present. A final distillation was affected from an all Pyrex glass system with a large cross-section vapor path to avoid splashing. The water was stored in an aged Pyrex bottle with ground glass joints and a glass siphon for removal of the water when needed. Ascarite in a U-tube scrubbed the air which entered the storage vessel as water was removed. The surface tension of the water was measured by the ring method using a DuNouy tensiometer. Values to within about 0.2 dyne per cm. of the literature values were always found.

The mercury used in the experiment was Goldsmith Brothers triply distilled grade. Oxygen was bubbled through the mercury while it was covered with a solution of sodium hydroxide. The metals removed by this procedure are Na, Mg, Rb, Zn, Cd, Sn, Pb, and Tl (23). After washing with distilled water the mercury was allowed to stream from a separatory funnel into the open end of a five foot column packed with glass beads and

filled with 0.001 M nitric acid on the first pass, 0.01 M on the second, and 1 M on the third pass. The beads dispersed the mercury and produced a tortuous and lengthy path for the descent of the small droplets. A continually renewed surface was thus brought into contact with the acid solutions and optimum conditions were realized for extracting traces of Mg, Al, Cr, Mn, Cd, Ni, Sn, Pb, and Cu. Vacuum distillation in an all Pyrex glass system concluded the mercury purification procedure. Platinum, Ag, and Cu are removed by this step in addition to Sn, Pb, Zn, and Cd not previously removed by the preceding chemical steps.

The perchloric acid used was Baker and Adamson C. P. Reagent Grade material. The only purification procedure was a distillation under reduced pressure. The fraction collected for use boiled at 70.0 - 70.5°C. There was no attempt to measure the pressure in the system during the distillation. The perchloric acid was stored in a Pyrex flask equipped with ground glass stopper.

Hydrogen used to provide an inert atmosphere as described later, was Balbach commercial grade, 99.8 per cent pure with the known impurities listed as water. To remove traces of oxygen, the hydrogen was passed over copper turnings maintained at 450°C. Water formed in this process and the water initially present was condensed and frozen in a trap maintained at -79°C by an acetone bath cooled with solid carbon dioxide. A

De-oxo Catalytic Purifier in which the agent was finely divided palladium further reduced the oxygen content of the stream. Two traps cooled by liquid nitrogen removed traces of other impurities.

Potassium perchlorate was Baker and Adamson C. P. Reagent Grade material. It was twice recrystallized from conductivity water and stored above anhydrous magnesium perchlorate to dry.

Platinum used in various parts of the apparatus was from Metals and Controls, Inc., and listed as pure.

Gold used in the preparation of the mercury electrode cup was in the form of Fine Gold wire of 1/16 inch diameter purchased from Engelhard Industries, Inc.

A solution or suspension of a platinum salt in an organic medium was purchased from Hanovia Chemical and Manufacturing Co. as Liquid Bright Platinum No. 05. The composition was unknown.

Other chemicals used in the investigation were Baker and Adamson C. P. Reagent Grade or equivalent. No further purification was required for these materials.

Preparation of Solutions

An aqueous solution of perchloric acid was prepared by dilution of the acid purified by the procedure already described with the conductivity water whose treatment has likewise been described. One hundred milliliters of the acid

diluted to 1000 milliliters had a concentration of 1.15 M as determined by titration with standard base solution.

A solution 0.05 M in potassium perchlorate and 10^{-5} M in perchloric acid was prepared by saturating conductivity water maintained at 0°C with purified potassium perchlorate and adding 10^{-2} milliliters of the 1.15 M perchloric acid.

A platinizing solution was prepared according to Jones and Bullinger (24). A 3 per cent solution was prepared by the addition of sufficient 6 M HCl solution to 3 grams of chloroplatinic acid to dissolve the salt in 50 milliliters of conductivity water. The resulting solution was diluted to 100 milliliters after addition of 0.03 grams of lead acetate.

A solution 0.05 M in potassium perchlorate was prepared by saturating conductivity water with the purified salt at 0.2°C. The solution was made 10^{-5} M in perchloric acid by the addition of 0.01 milliliter of 1.15 M perchloric acid to 1 liter of the potassium perchlorate solution.

The Cell

The container for the solution was formed from a 55/60 Pyrex double walled standard taper, outer. The ring seal at the bottom completed a thermostatting jacket through which water from constant temperature source could be circulated. The temperature of a solution in the cell could be maintained constant within limits of ± 0.25 near 0°C.

At A in Figure 1, a 55/60 Pyrex standard taper, inner, closed the cell against the atmosphere and served as a support for the various components of the cell. B is a gas dispersing tube ring-sealed to a 19/20 Pyrex standard taper joint, inner, with a Teflon-plug stopcock at C for by-passing the gas disperser. When the stopcock was closed, hydrogen bubbled through the solution. When the stopcock was open, the bubbler was inoperative but an atmosphere of hydrogen was maintained above the solution without sweeping large volumes of hydrogen over the surface of the solution, thus avoiding extensive evaporation.

At D is a standard taper, outer, having a small reservoir filled with mercury and making electrical contact with the outside of the cell through a platinum wire leading through the bottom of the reservoir to a second mercury filled cup into which a platinum wire could be dipped from the outside. Into the standard taper at D fitted an inner joint to which was sealed the reference electrode, E. This arrangement proved convenient when it was necessary to clean the cell or replatinize the reference electrode. The position of the reference electrode with respect to the mercury electrode was easily reproduced.

F is a Pyrex tube ring sealed to the support taper A. F supports the mercury reservoir and mercury electrode. Through F leads a 1/16 inch platinum rod, G, with a 1/4 inch diameter

Figure 1. Schematic of cell on which measurements were made

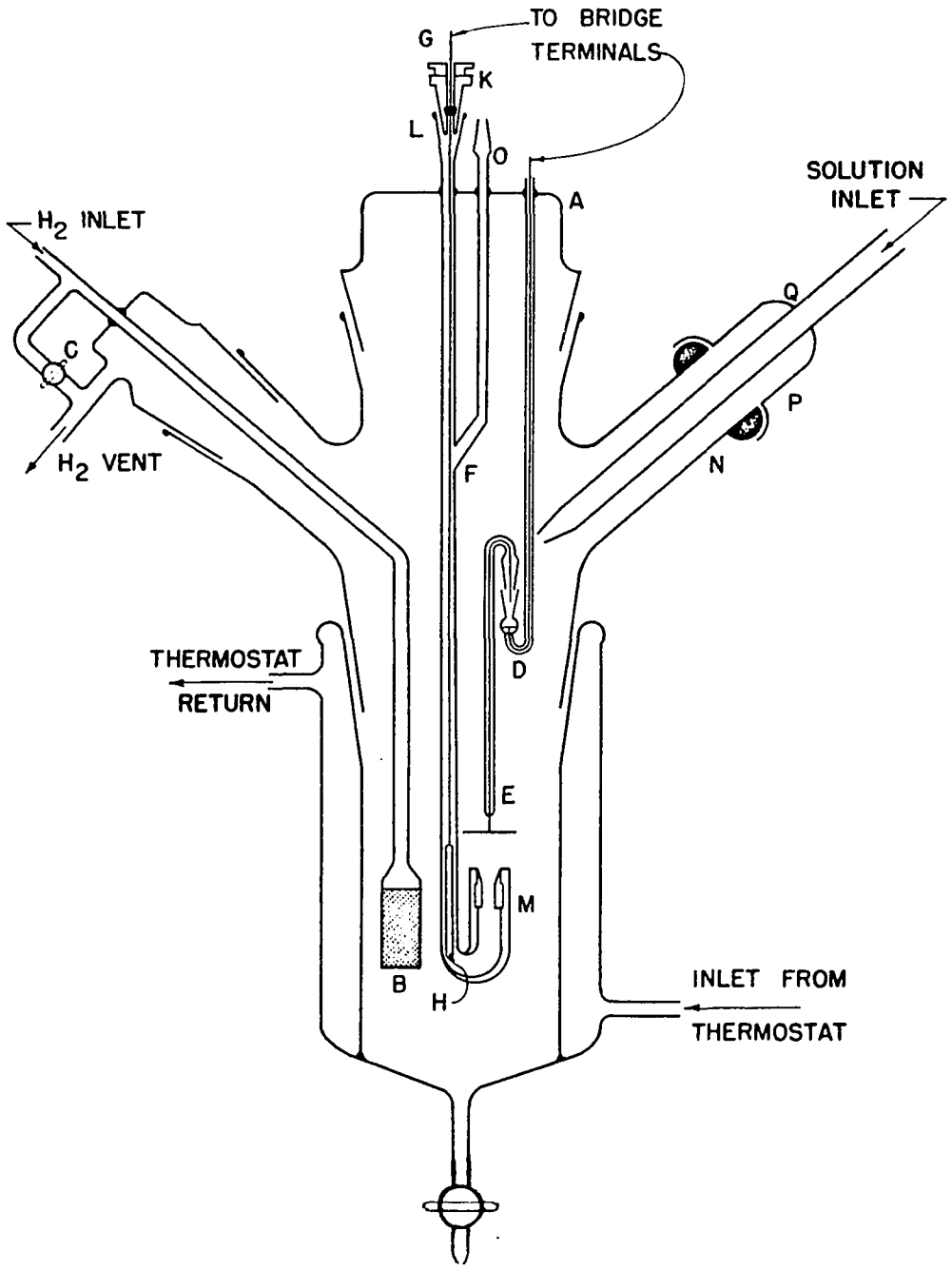
TO BRIDGE
TERMINALS
G
K
L
O
A
SOLUTION
INLET
H_2 INLET
Q
C
P
H_2 VENT
F
N
D
THERMOSTAT
RETURN
E
M
B
H
INLET FROM
THERMOSTAT

platinum bob, H, about two inches long. The upper end of G was threaded along about four inches of its length and a matching platinum nut could be screwed over the end. The rod G was inserted through a Teflon plug, K, the outside of which had been machined to fit tightly the 12/30 Pyrex standard taper, outer, at L. The platinum nut was then screwed on the end of G and a threaded Teflon sleeve inserted into K and screwed tight. The nut was firmly held in place so that the bob, H, could be raised or lowered by turning G. The level of the mercury electrode at M could be easily adjusted to give a plane interface between the mercury and the solution. An expanded view of the Teflon plug is shown in Figure 2.

Mercury could be introduced into the reservoir through the standard taper at O. A ring-seal through the support taper, A, led a glass tube to the interior of the cell where a T-seal was made to F. The taper at O could be connected to the hydrogen exit port of the cell to maintain equal pressure on both sides of the mercury at all times. By loosening the Teflon plug K, the mercury reservoir could be flushed with hydrogen after each addition of mercury.

A ball joint at N served as the entry port for solutions. A socket 18/9 with a ring seal at Q about two inches from the end connected the cell to the solution reservoir. The solution reservoir could be pressurized with hydrogen and solution forced through connecting glass tubing to the cell. The ring

Figure 2. Teflon standard taper in cross-section. Shown are platinum rod and nut by means of which mercury level was controlled

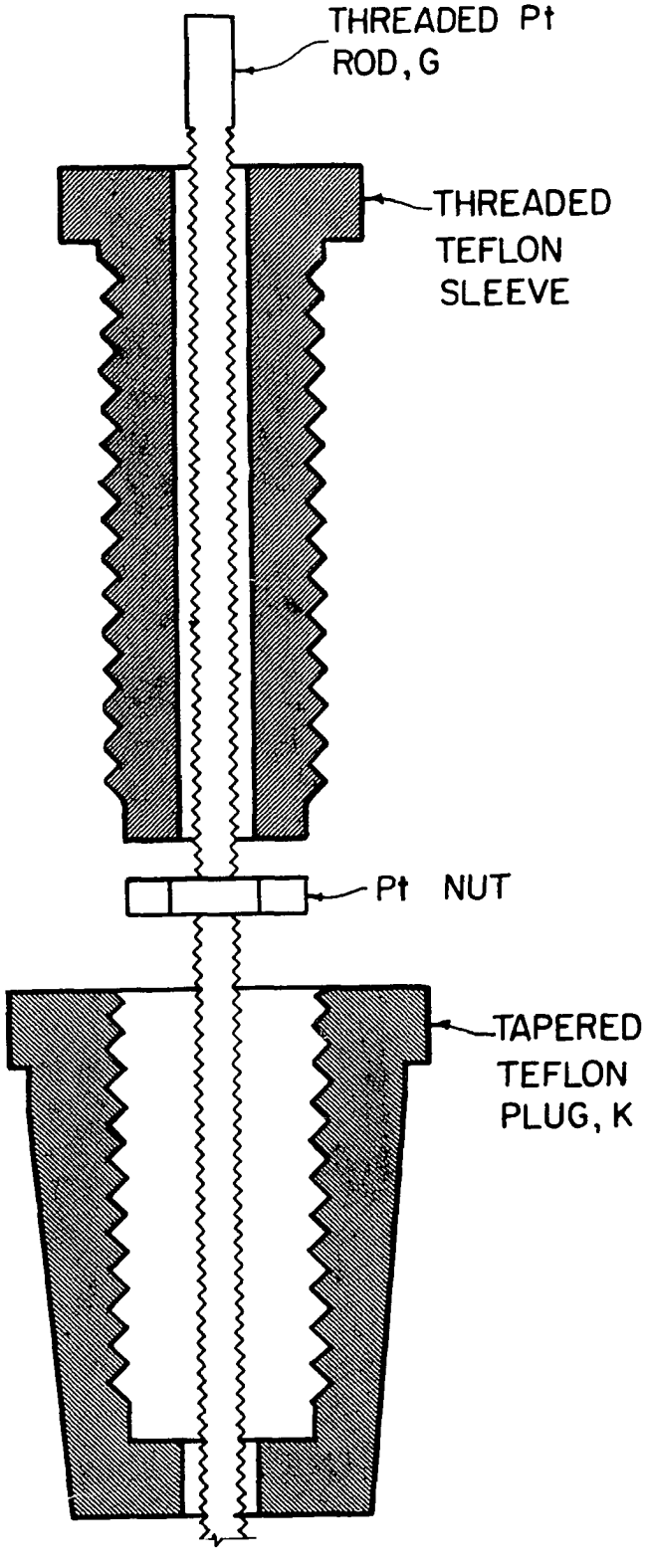
THREADED Pt
ROD, G
THREADED
TEFLON
SLEEVE
Pt NUT
TAPERED
TEFLON
PLUG, K

seal at Q permitted the solution to be led past the socket N and into the cell without wetting the joint with solution.

Three mercury electrodes were used in this investigation. For convenience they will be designated electrode I, electrode II, electrode III, as pictured in Figure 3. Electrode I was constructed from Pyrex glass capillary tubing with an outside diameter of about 6 millimeters and an inside diameter of 2.1 millimeters. The inside diameter was determined as an average of four diameters measured at as many orientations using a Cambridge Universal Measuring Machine. The maximum deviation of the measurements from the average was 0.01 millimeters. The preparation of the electrode was as follows. Liquid Bright Platinum No. 05 was introduced in a section of a capillary and spread uniformly over the interior of the capillary by inclination of the capillary to allow the one or two drops of "Liquid Platinum" to flow along the inside of the tube. The capillary was tilted and rotated successively until the coating gave the appearance of a uniform thickness. Care was taken to prevent the solution from coating the polished end of the capillary. The capillary was clamped in a vertical position and a stream of dry air was passed slowly through the tube from the bottom. After several hours of this air drying, the tube was transferred to an oven maintained at 115°C and dried for two more hours. The final firing to reduce the platinum salt was at 675°C. This temperature was maintained for only about five

Figure 3. Electrode designs in cross-section

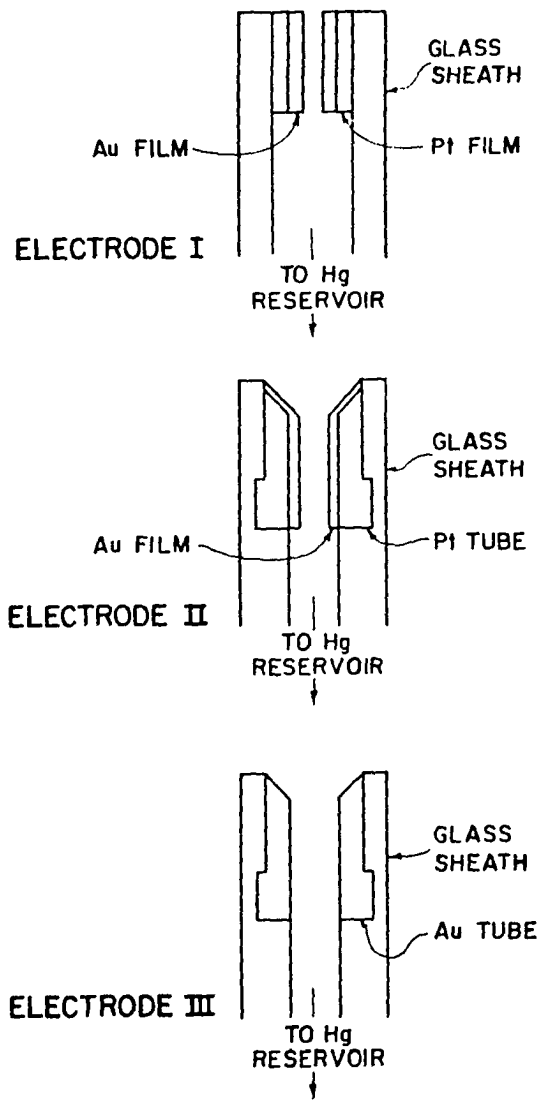
GLASS SHEATH
Au FILM
Pt FILM
ELECTRODE I
TO Hg RESERVOIR
GLASS SHEATH
Au FILM
Pt TUBE
ELECTRODE II
TO Hg RESERVOIR
GLASS SHEATH
Au TUBE
ELECTRODE III
TO Hg RESERVOIR

minutes so that no distortion of the capillary occurred even though the annealing temperature for Pyrex is about 550°C. The interior of the capillary was left with a thin mirror bright film of platinum. Gold was electroplated onto the platinum film from the end of the capillary to about 0.5 centimeter removed from the end. The platinum film served as cathode while a platinum wire centered in the capillary served as anode. About 0.5 milliamperes were passed until a visible deposit of gold resulted. It is estimated that not more than 0.2 milligrams of gold were deposited. This capillary could then be sealed to the mercury reservoir in the position shown in Figure 1. Electrodes prepared in this manner proved to be short-lived and difficult to construct.

Electrodes of type II were constructed by machining a short section of 1/8 inch platinum rod to a diameter of approximately 0.045 inch, forming a shoulder. The machined section of the rod was about 0.12 inch in length. The rod was cut off to give a total length of approximately 0.20 to 0.30 inch. A hole 0.025 inch in diameter was drilled along the axis of the cylinder. The cylinder was then inserted in a Pyrex capillary one end of which had been sealed by fusing the glass. The open end of the capillary was then connected to a vacuum pump and the air exhausted while the capillary and platinum cylinder were heated to 450°C. After about two hours of heating under vacuum the capillary was removed from the

furnace and a hand torch was used to heat the glass near the closed end. The pressure differential across the capillary walls collapsed the softened glass onto the platinum cylinder. By heating progressively from the end, collapse was initiated from the end of the capillary and progressed along it to a point just short of the large end of the platinum tube. The capillary with the tube sealed in place was returned to the furnace, now at 550°C, and kept at this temperature for about ten minutes and then cooled slowly to room temperature. After cooling, the mass of glass sealing the end of the capillary was cut off perpendicular to the longitudinal axis of the tube and flush with the end of the platinum tube. After polishing the end of the capillary with fine abrasive paper, a machinist's drill bit of 0.055 inch in diameter was used to bevel the inside of the platinum tube to give a knife edge in the plane of the polished end of the capillary. This operation was observed through a binocular microscope of magnification 12. The drill bit was rotated by hand and care was taken to insure that no chipping of the glass occurred around the edge of the tube. The thickness of the edge produced was too small to be measured with a reticle on the microscope. The final operation in preparation of the electrode was electroplating a thin film of gold onto the beveled portion of the tube, using the same technique as that described for electrode I. The precision of capacity measurements on this electrode was poor

and hydrogen evolution could be observed at the edges upon negative polarization of the electrode.

Electrode III was constructed by sealing a gold tube in a glass capillary just as described for electrode II. The capillary diameter and the diameter of the gold tube were about the same as for the platinum tube. There was no need for the final electroplating step described for electrode II. This was found to give reproducible results and small negative polarizations were possible without hydrogen evolution.

The reference electrode was made from a disc of platinum foil 0.003 inch in thickness and one inch in diameter. A platinum wire was spot welded to the center of the disc and a short length of Pyrex tubing was sealed to the wire near the disc. A 5/7 standard taper inner was sealed to the other end of the glass tube and the wire led through the taper. A sharp U-bend was made in the sheath for the wire so that the taper axis was parallel to the axis of the glass sheath with the taper diameter decreasing toward the disc. The wire leading through the sheath and out the standard taper was long enough to extend 1/8 inch beyond the end of the taper.

The disc was platinized by passing a direct current of about 0.3 amperes across it for ten minutes while immersed in the platinizing solution previously prepared. A second disc of about the same size completed the circuit through the solution. A Flex-O-Pulse Timer and a mechanical relay served to

reverse the polarity at the electrodes once every thirty seconds.

The solution reservoir (Figure 4) was a 500 milliliter Erlenmeyer flask with a standard taper outer sealed to the neck. A platinum wire sealed through the bottom of the flask made electrical contact to a pool of mercury in the bottom of the flask. A standard taper inner served as a support for a rectangular platinum electrode extending to about two centimeters above the mercury pool. The support taper also had an entry for hydrogen sealed to it and an exit tube extending to within two millimeters of the mercury pool. The exit tube conducted solution out of the reservoir through a ball and socket joint with a ring seal similar to N, P, Q in Figure 1. Hydrogen purified as previously described could be diverted from the cell proper to the solution reservoir by means of the three way Teflon stopcock shown.

Electronic Apparatus

The bridge for use in the measurements reported here was constructed around a Leeds and Northrup shielded ratio box, catalog number 1553. A shielded step-down transformer is incorporated in this ratio box. Shielded binding posts made connections to the various external pieces of equipment.

The input signal to the transformer in the ratio box was supplied by a Hewlett Packard Model 200CD wide range oscilla-

Figure 4. Pre-electrolysis cell

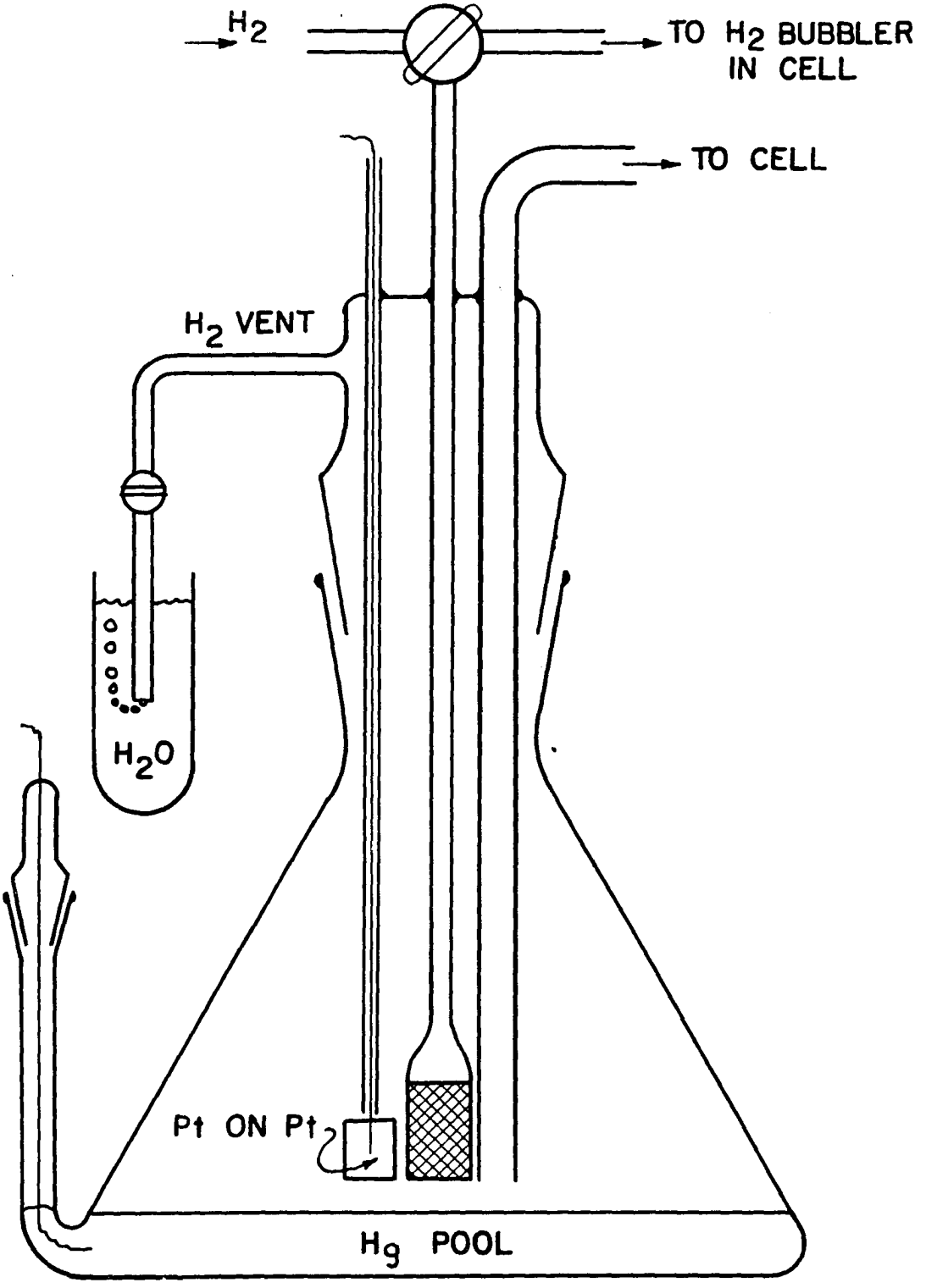
H2
TO H2 BUBBLER IN CELL
TO CELL
H2 VENT
H2O
Pt ON Pt
Hg POOL

tor. The signal from the oscillator was attenuated by using a simple potential dividing device constructed from precision resistors. This permitted operation of the oscillator at a high output level where best frequency stability was observed while utilizing a low level signal for the operation of the bridge.

The measuring arm of the bridge consisted of a Freed Transformer Co. Model 1350 decade capacitor and a non-inductively wound Leeds and Northrup Co. decade resistance, catalog number 4764, in series connection. The lowest capacity range was covered by a continuously variable air capacitor with a maximum value of 1000 micro-microfarads and a scale calibrated in units of 10 micro-microfarads. Four decades in units of 0.001 microfarad, 0.01 microfarad, 0.1 microfarad, and 1 microfarad extended the range of the decade capacitor to 11 microfarads. The decade resistance had six units variable in increments of 0.01, 0.1, 1, 10, 100, and 1000 ohms, respectively, and covering the range from 0.01 ohm to 11,000 ohms. Contact resistances were negligible in both of these circuit elements and the reproducibility in settings were consequently limited only by other factors in the measurement.

A second pair of elements like the above were used in the substitution procedure to be described later. The connections to this cell analog were made as nearly identical with those to the cell proper as could be achieved.

The null detector for the bridge was based on a DuMont Type 304-H cathode ray oscilloscope with both X and Y input terminals. The output signal from the bridge was of such low level that amplification was necessary prior to display on the cathode ray oscilloscope screen. The bridge output was first amplified by a Hewlett Packard wide band amplifier, Model 450A, operating at a gain of 100 to 1. This signal was in turn amplified by a twin-tee narrow band amplifier designed and constructed in this laboratory. A schematic diagram showing 33 1/3 cycles per second tees is presented in Figure 5. Pairs of tees used in the measurements were constructed for use at nominal frequencies of 100, 250, 500, 750, 1000, 2500, 5000, 10,000 cycles per second. The filtered, amplified signal from the twin tee produced the Y displacement on the cathode ray oscilloscope screen.

To gain some additional sensitivity in the measurements, a phase sensitive technique was used. A second Hewlett Packard Model 450A wide band amplifier was connected to the bridge so that the input signal to the bridge could be amplified and used to produce the X deflection on the cathode ray oscilloscope screen. Thus, a series of Lissajou's figures showed the amplitude of the output signal from the bridge and the phase of this signal with respect to the input. A horizontal straight line indicated a balance condition. The X axis of the cathode ray oscilloscope was calibrated and used

Figure 5. Twin tee amplifier circuit in schematic form shown with 33 1/3 cycles per second tees

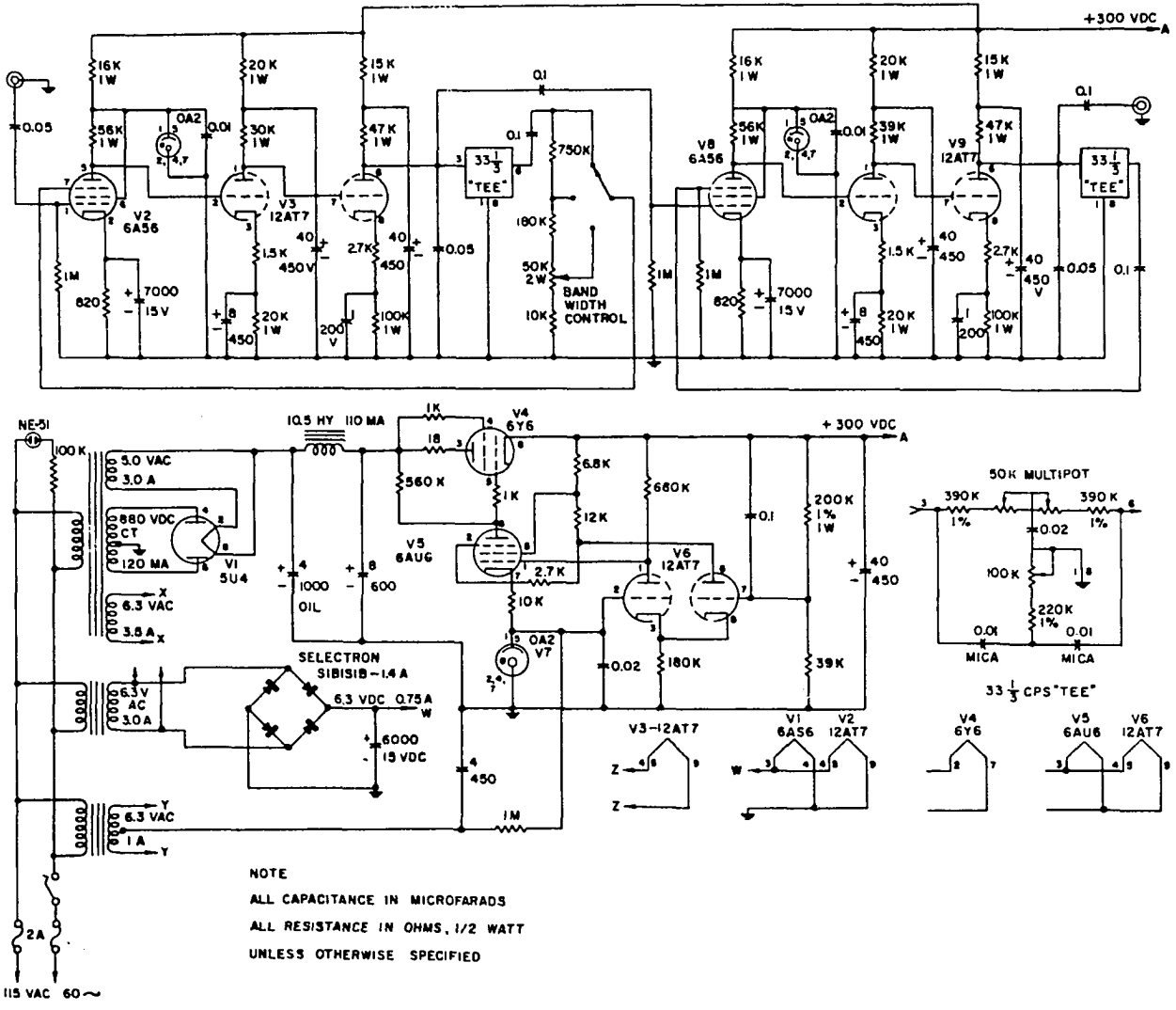

NOTE

ALL CAPACITANCE IN MICROFARADS

ALL RESISTANCE IN OHMS, 1/2 WATT

UNLESS OTHERWISE SPECIFIED

to measure the input signal to the bridge.

A Rubicon, Type B, high precision potentiometer was used to polarize the mercury electrode of the cell. Two six volt storage batteries supplied current to the potentiometer. The potentiometer slide wire was calibrated against an Eppley Laboratories standard cell, catalog number 100. A Rubicon galvanometer, catalog number 3411, with a sensitivity of 1.5 microvolts per millimeter was used in the calibration. A switch was arranged for direct connection of the galvanometer terminals on the potentiometer after the calibration procedure was completed. The potentiometer was completely enclosed in a grounded metal box for shielding.

A Simpson microammeter with a full scale deflection of $\pm$ 25 x 10^{-6} amperes was connected in series with the cell and potentiometer to detect and measure any direct current in the system.

All electrical connections were made with high quality shielded cables. The cell itself was enclosed in a grounded copper screen box.

Figure 6 is a schematic of the bridge including a Model 225C Computer Measurements counter to monitor frequency.

Procedure

The cell components were cleaned by immersion for several hours in a hot mixture of nitric and sulfuric acids. The various pieces were washed thoroughly with conductivity water

Figure 6. Bridge circuit in schematic showing accessory equipment in block diagram

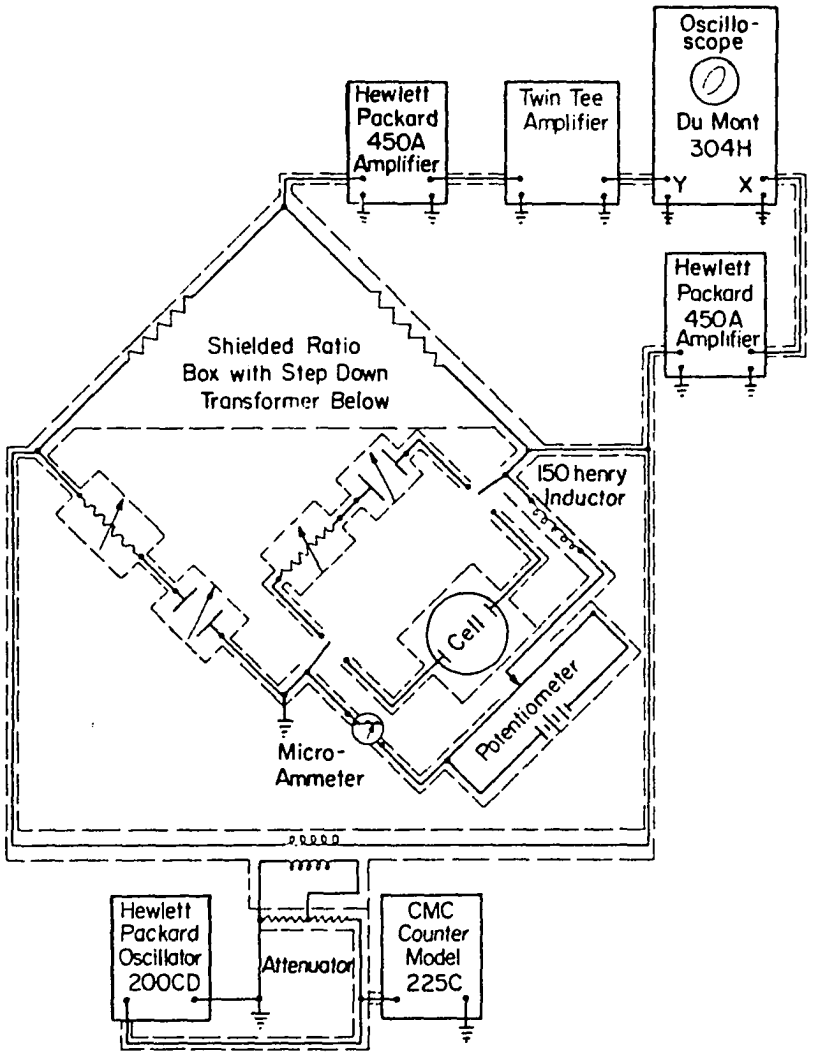
Oscillo-
scope
Du Mont
304H
Y
X
Hewlett
Packard
450A
Amplifier
Twin Tee
Amplifier
Hewlett
Packard
450A
Amplifier
Shielded Ratio
Box with Step Down
Transformer Below
150 henry
Inductor
Cell
Potentiometer
Micro-
Ammeter
Hewlett
Packard
Oscillator
200CD
Attenuator
CMC
Counter
Model
225C

upon removal from the acid bath and then dried at 150°C.

While the cleaning of the cell was underway, the solution to be used in the measurements was placed in the solution reservoir and a direct current of about 100 milliamperes passed through the solution with the mercury pool in the bottom as anode. This pre-electrolysis was helpful in reducing the rate at which the capacitance changed with time. The minimum time which seemed to be effective was twelve hours. In all cases reported here, the pre-electrolysis lasted for twenty hours or more.

The clean cell was assembled and mercury added to the U-tube reservoir connecting to the mercury electrode. Hydrogen was admitted to the solution reservoir and solution was forced out of the reservoir to the cell. After filling to a level some 2 to 3 centimeters above the reference electrode, hydrogen was diverted from the solution reservoir and bubbled through the solution in the cell for at least two hours. Removal of dissolved air and establishment of thermal equilibrium were the objects of this step.

The potentiometer was standardized and the mercury in the electrode was leveled by adjusting the height of the platinum bob in the mercury reservoir. The potentiometer was set to give the desired potential and the leads to the two electrodes of the cell were connected. The output of the oscillator was adjusted to the proper frequency and the capacity and resist-

ance in the balancing arm were adjusted to give a minimum trace on the cathode ray oscilloscope screen. Without renewing the mercury surface or changing the potential applied to the surface, measurements were made at other frequencies by changing the several tees in the high gain amplifier and changing the output frequency of the oscillator. After completing a frequency scan at a given potential, the potential was changed, the mercury surface renewed, and the procedure was repeated. The frequency of the signal was always determined with the counter to four significant figures and the frequencies measured during use of a particular pair of tees could be adjusted to the same value within limits of $\pm$ 0.3 cycles per second at 100.0 cycles per second and within limits of $\pm$ 5 cycles per second at 9055 cycles per second.

The cell impedance was measured as a function of applied potential and of frequency for temperatures of 0.5°C, 24.7°C, and 55.0°C. Hydrogen evolution became a problem for negative polarizations of the mercury. For this reason, 1.15 M perchloric acid was mainly used only for measurements with the mercury positive with respect to the electrocapillary maximum. The potential for reversible hydrogen evolution is somewhat negative with respect to the electrocapillary maximum if the hydrogen ion concentration is about 10^{-5}. To obviate the hydrogen evolution problem, measurements of the impedance for negative potentials were on 0.05 M $KClO_4$, 10^{-5} M $HClO_4$.

A substitution technique was used to eliminate effects due to asymmetries in the bridge network and in the electrical leads. The cell was replaced by a series combination of a decade resistance with a decade capacitance. This cell analogue combination became the adjustable arm of the bridge in the calibration procedure. The resistance and the capacitance which initially balanced the cell impedance were in turn balanced by adjusting the resistance and capacitance in the analogue. By using identical shielded electrical leads for connecting both the cell and the analogue to the bridge terminals, the identity of the impedance of the analogue with that of the cell was insured.

RESULTS AND DISCUSSION

The results of measurements of capacity and resistance as a function of polarization and frequency are presented for three temperatures and two solutions in Tables 1 to 12. Graphical displays of the data are shown in Figures 7 to 18. Both resistance and capacity are seen to be markedly frequency dependent but there is little change in the character of the curves showing this dependence as the polarization changes. The object of this research was to explain this dependence, whether due to experimental design or to basic properties of the interfacial region. We begin the discussion of these data in terms of a rather attractive theory which has previously been proposed.

Polar molecules in an external electric field experience a force tending to produce orientation of the dipole axis parallel with the electric field. In the absence of any but dipole interactions between molecules one should expect the dipole orientation to change instantaneously when the direction of the field is abruptly altered. That is to say, the field direction and the dipole axis would be in phase. Sudden reduction of an external field to zero should be accompanied by an equally rapid decrease of the polarization of the medium to zero. In practice, such behavior is not observed. A static field applied to a dielectric generally produces a

Table 1. Capacity of mercury-aqueous interface for 1.15 M $HClO_4$ for several signal frequencies and several polarizations of the mercury at 0.5°C[a]

E	Frequency							
	100	255	505	754	997	2425	4890	9060
-0.300	571	515	480	463	453	427	409	392
-0.200	602	548	512	494	483	456	437	419
-0.100	659	597	560	541	529	499	478	458
+0.100	498	449	415	400	392	370	357	342
+0.200	518	465	432	416	-	382	367	352
+0.300	548	490	455	437	429	402	385	369
+0.400	575	515	481	464	454	426	408	391
+0.500	606	548	512	495	484	455	436	420
+0.600	666	603	567	547	535	504	481	461

[a]Capacity in millimicrofarads. Polarizing potential, E, in volts relative to a hydrogen electrode at 0.5°C. Frequency in cycles per second. Electrode Area - 0.01156 $cm.^2$.

polarization which requires a time lapse for equilibrium to be established. Viscous forces between spherical dipoles might be the source of a time lag between application of a field and the steady state polarization resulting from it.

Debye (25) has treated this problem for static fields and for periodic fields. He calculates a distribution function describing the orientation of dipoles in an electric field. This function is used to determine the mean electric moment

Table 2. Capacity of mercury-aqueous interface for 1.15 M perchloric acid for several signal frequencies and several polarizations of the mercury at 25°C[a]

E	Frequency							
	100	255	505	754	997	2425	4890	9060
+0.602	625	567	533	518	506	475	453	436
+0.552	532	500	480	470	461	437	421	405
+0.502	493	467	450	441	434	412	395	381
+0.452	467	445	431	423	415	394	379	366
+0.400	452	431	415	410	401	382	367	355
+0.350	428	408	395	390	383	368	357	343
+0.300	414	396	385	379	373	357	345	334
+0.250	402	-	371	367	361	347	335	325
+0.200	392	375	363	360	353	340	329	318
+0.150	386	368	357	355	348	335	324	314
+0.100	363	349	339	336	333	323	316	306
+0.050	368	356	346	343	339	329	321	313
0.000	373	359	350	347	343	333	325	317
-0.050	376	363	355	352	348	339	332	323
-0.100	394	381	372	365	361	346	337	328

[a]Capacity in millimicrofarads. Polarizing potential, E, in volts relative to a hydrogen electrode at 25°C. Frequency in cycles per second. Electrode area - 0.01156 $cm.^2$.

Table 3. Capacity of mercury-aqueous interface for 1.15 M $HClO_4$ for several signal frequencies and several polarizations of the mercury at 54.7°C[a]

E	Frequency							
	100	255	505	754	997	2425	4890	9060
+0.100	506	477	457	445	436	413	388	370
+0.200	536	506	480	466	454	424	400	381
+0.300	582	538	508	490	478	443	419	399
+0.400	615	573	540	521	508	471	446	424
+0.500	679	635	600	580	566	527	494	466

[a]Capacity in millimicrofarads. Polarizing potential, E, in volts relative to a hydrogen electrode at 54.7°C. Frequency in cycles per second. Electrode Area - 0.01156 $cm.^2$.

Table 4. Capacity of mercury-aqueous interface for 0.05 M $KClO_4$ - 10^{-5} M $HClO_4$ for several signal frequencies and several polarizations of the mercury at 0.5°C[a]

E	Frequency							
	100	255	505	754	997	2425	4890	9060
0.000	637	598	556	541	528	468	396	316
-0.100	457	428	409	398	390	349	298	244
-0.200	409	384	367	359	351	316	274	227
-0.300	378	357	341	332	325	292	253	212
-0.400	371	349	333	324	317	284	247	209
-0.500	387	364	348	338	330	296	262	222

[a]Capacity in millimicrofarads. Polarizing potential, E, in volts relative to a hydrogen electrode at 0.5°C. Frequency in cycles per second. Electrode Area - 0.01156 $cm.^2$.

Table 5. Capacity of mercury-aqueous interface for 0.05 M $KClO_4$ - 10^{-5} M $HClO_4$ for several signal frequencies and several polarizations of the mercury at 25°C[a]

E	Frequency							
	100	255	505	754	997	2425	4890	9060
0.000	580	536	513	498	490	451	405	350
-0.100	481	451	430	419	411	381	342	298
-0.200	440	-	396	386	378	351	316	277
-0.300	408	383	367	358	351	326	297	266
-0.400	391	368	354	343	337	312	283	253
-0.500	394	373	357	347	340	315	288	258

[a]Capacity in millimicrofarads. Polarizing potential, E, in volts relative to a hydrogen electrode at 25°C. Frequency in cycles per second. Electrode Area - 0.01156 $cm.^2$.

Table 6. Capacity of mercury-aqueous interface for 0.05 M $KClO_4$ - 10^{-5} M $HClO_4$ for several signal frequencies and several polarizations of the mercury at 54.7°C[a]

E	Frequency							
	100	255	505	754	997	2425	4890	9060
0.000	1022	889	794	751	735	605	552	488
-0.100	545	501	471	455	443	404	357	309
-0.200	463	411	431	397	387	362	330	299
-0.300	425	399	382	372	365	340	311	280
-0.400	411	387	369	359	354	333	298	267
-0.500	375	356	339	329	322	307	289	261

[a]Capacity in millimicrofarads. Polarizing potential, E, in volts relative to a hydrogen electrode at 54.7°C. Frequency in cycles per second. Electrode Area - 0.01156 $cm.^2$.

Table 7. Cell resistance associated with double layer capacity for 1.15 M $HClO_4$ for several signal frequencies and several polarizations of the mercury at 0.5°C[a]

E	Frequency							
	100	255	505	754	997	2425	4890	9060
-0.300	491.5	262.9	106.6	74.03	58.11	31.27	23.08	19.48
-0.200	439.3	188.3	98.68	68.94	54.45	30.08	22.42	19.08
-0.100	411.2	174.1	91.04	63.87	50.91	28.85	21.93	18.77
+0.100	569.6	241.2	123.83	84.88	66.14	34.26	24.44	20.46
+0.200	568.4	239.3	121.50	83.04	-	33.60	24.20	20.17
+0.300	553.5	229.8	117.5	80.31	62.71	33.13	24.11	20.20
+0.400	513.5	212.9	109.51	75.28	59.06	31.88	23.46	19.85
+0.500	462.8	190.7	100.46	69.95	55.33	30.72	23.02	19.66
+0.600	410.5	171.7	90.60	63.94	51.04	29.28	22.30	19.19

[a]Resistance in ohms. Polarizing potential, E, in volts relative to a hydrogen electrode at 0.5°C. Frequency in cycles per second. Electrode Area - 0.01156 $cm.^2$

Table 8. Cell resistance associated with electrode capacity for 1.15 M perchloric acid for several signal frequencies and several polarizations of the mercury at 25°C[a]

E	Frequency							
	100	255	505	754	997	2425	4890	9060
+0.602	551.2	186.15	90.20	61.42	48.60	25.61	17.80	14.29
+0.552	468.5	151.7	78.37	52.86	44.05	24.37	17.50	14.11
+0.502	434.2	147.2	75.77	51.45	44.31	24.88	17.86	14.41
+0.452	377.5	136.4	73.94	51.47	43.74	25.10	18.05	14.54
+0.400	476.0	154.0	79.14	53.86	45.17	25.56	18.17	14.56
+0.350	408.0	138.0	73.70	45.35	42.21	24.51	17.89	14.57
+0.300	344.0	144.6	76.00	48.25	43.10	24.84	18.09	14.70
+0.250	418.0	-	75.60	50.11	42.50	24.41	17.88	14.58
+0.200	395.0	134.0	75.45	45.57	42.25	24.44	18.02	14.71
+0.150	405.0	146.40	76.00	47.14	46.30	24.63	18.00	14.67
+0.100	385.0	129.7	65.55	45.79	38.00	22.63	17.10	14.31

[a]Resistance in ohms. Polarizing potential, E, in volts relative to a hydrogen electrode at 25°C. Frequency in cycles per second. Electrode Area - 0.01156 $cm.^2$.

Table 8 (Continued).

E	Frequency							
	100	255	505	754	997	2425	4890	9060
+0.050	325.0	120.50	61.38	40.29	36.25	-	16.83	14.20
+0.000	379.0	126.7	62.97	41.63	36.30	23.21	16.72	14.17
-0.050	306.7	113.20	58.39	37.72	34.58	21.09	16.43	13.93
-0.100	272.0	120.3	68.67	45.84	40.83	23.16	16.44	13.82

Table 9. Cell resistance associated with double layer capacity for 1.15 M $HClO_4$ for several signal frequencies and several polarizations of the mercury at 54.7°C[a]

E	Frequency							
	100	254	505	754	997	2425	4890	9060
+0.100	434.4	166.1	91.00	65.52	52.63	27.31	17.98	13.55
+0.200	451.2	175.8	94.54	67.93	53.21	27.15	17.74	13.44
+0.300	420.5	175.8	94.25	66.58	52.58	26.91	17.40	13.19
+0.400	432.5	165.3	88.98	63.24	50.00	25.71	16.85	12.89
+0.500	398.0	147.7	80.69	58.29	45.92	25.23	16.94	12.96

[a]Resistance in ohms. Polarizing potential, E, in volts relative to a hydrogen electrode at 54.7°C. Frequency in cycles per second. Electrode Area - 0.01156 $cm.^2$.

Table 10. Cell resistance associated with double layer capacity for 0.05 M $KClO_4$ - 10^{-5} $HClO_4$ for several signal frequencies and several polarizations of the mercury at 0.5°C[a]

E	Frequency							
	100	255	505	754	997	2425	4890	9060
0.000	1392	1165.6	1094.40	1072.0	1062.1	1040.5	1028.6	1020
-0.100	1433	1198.6	1122.1	1096.6	1085.2	1059.7	1045.8	1033.3
-0.200	1471	1209.8	1126.8	1100.3	1088.4	1061.9	1045.6	1033.3
-0.300	1512	1225.8	1137.2	1108.5	1095.2	1065.6	1047.3	1034.5
-0.400	1516	1234.5	1146.2	1117.0	1102.9	1069.8	1049.5	1037.5
-0.500	1459	1217.8	1136.8	1108.7	1094.2	1059.7	1040.0	1029.3

[a]Resistance in ohms. Polarizing potential, E, in volts relative to a hydrogen electrode at 0.5°C. Frequency in cycles per second. Electrode Area - 0.01156 $cm.^2$.

Table 11. Cell resistance associated with double layer capacity for 0.05 M $KClO_4$ - 10^{-5} M $HClO_4$ for several signal frequencies and several polarizations of the mercury at 25°C[a]

E	Frequency							
	100	255	505	754	997	2425	4890	9060
0.000	977	714.1	639.1	614.62	603.78	584.84	575.15	568.45
-0.100	953	725.0	650.8	625.58	613.55	591.76	580.80	572.70
-0.200	979	-	654.9	629.60	617.80	595.02	582.97	574.3
-0.300	1012	735	651.7	624.25	610.75	584.85	572.58	564.3
-0.400	1027	743.8	662.8	632.48	618.80	590.85	577.40	568.4
-0.500	1000	736.8	658.1	630.33	616.00	588.44	574.94	566.1

[a]Resistance in ohms. Polarizing potential, E, in volts relative to a hydrogen electrode at 25°C. Frequency in cycles per second. Electrode Area - 0.01156 $cm.^2$.

Table 12. Cell resistance associated with double layer capacity for 0.05 M $KClO_4$ - 10^{-5} M $HClO_4$ for several signal frequencies and several polarizations of the mercury at 54.7°C[a]

E	Frequency							
	100	255	505	754	997	2425	4890	9060
0.000	857	554.4	461.62	431.47	414.90	389.97	378.1	372.6
-0.100	825	569.8	485.05	457.35	441.25	413.51	400.74	391.39
-0.200	790	466.1	543.2	438.28	421.46	392.96	380.7	373.55
-0.300	803	541.9	465.4	440.84	425.80	399.39	386.62	379.75
-0.400	856	563.4	477.70	453.58	439.21	411.11	400.4	389.70
-0.500	847	549.5	467.1	439.42	424.22	396.47	384.27	376.98

[a]Resistance in ohms. Polarizing potential, E, in volts relative to a hydrogen electrode at 54.7°C. Frequency in cycles per second. Electrode Area - 0.01156 $cm.^2$.

for a system of dipoles and the molar polarization follows. Under the assumption of no internal field, the displacement then was calculated. For static fields, the treatment predicted an exponential time dependence of the displacement, building up to a steady value upon application of a field and decreasing to zero upon reduction of the field to zero, each process occurring with the same characteristic half-life or relaxation time. Time constants for RC circuits were shown to depend on the relaxation time of the dielectric material filling the condenser.

The same approach applied to the case of a dielectric in a periodic field led to the introduction of a complex dielectric constant, with real and imaginary parts both dependent on the period of the external field. When written as a complex number,

$$\epsilon = \epsilon' - i\epsilon'' \tag{12}$$

the frequency dependence of the dielectric constant is given by

$$\epsilon' - \epsilon_\infty = \frac{\epsilon_0 - \epsilon_\infty}{1 + \left(\frac{\epsilon_0 + 2}{\epsilon_\infty + 2}\right)^2 \omega^2\tau^2} \tag{13}$$

and

$$\epsilon'' = (\epsilon_0 - \epsilon_\infty)\left[\frac{\frac{\epsilon_0 + 2}{\epsilon_\infty + 2}\omega\tau}{1 + \left(\frac{\epsilon_0 + 2}{\epsilon_\infty + 2}\right)^2 \omega^2\tau^2}\right] \tag{14}$$

Figure 7. Double layer capacity as a function of frequency for mercury in 1.15 M $HClO_4$ at 0.5° C. Representative polarizations, E, relative to the hydrogen electrode at 0.5° C. Area of mercury electrode - 0.01156 cm^2

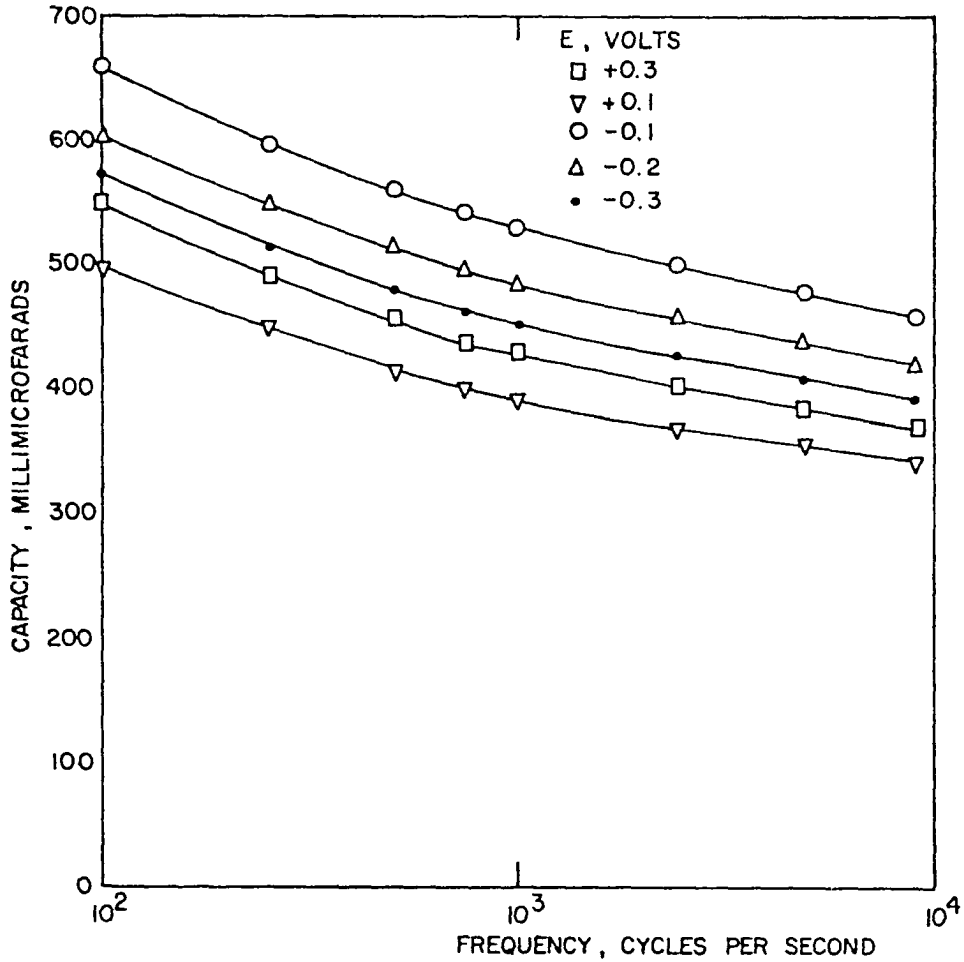
E, VOLTS
+0.3
+0.1
-0.1
-0.2
-0.3
700
600
500
400
300
200
100
0
CAPACITY, MILLIMICROFARADS
10^2
10^3
10^4
FREQUENCY, CYCLES PER SECOND

Figure 8. Double layer capacity as a function of frequency for mercury in 1.15 M $HClO_4$ at 25°C. Representative polarizations, E, relative to the hydrogen electrode at 25°C. Mercury electrode area - 0.01156 cm^2

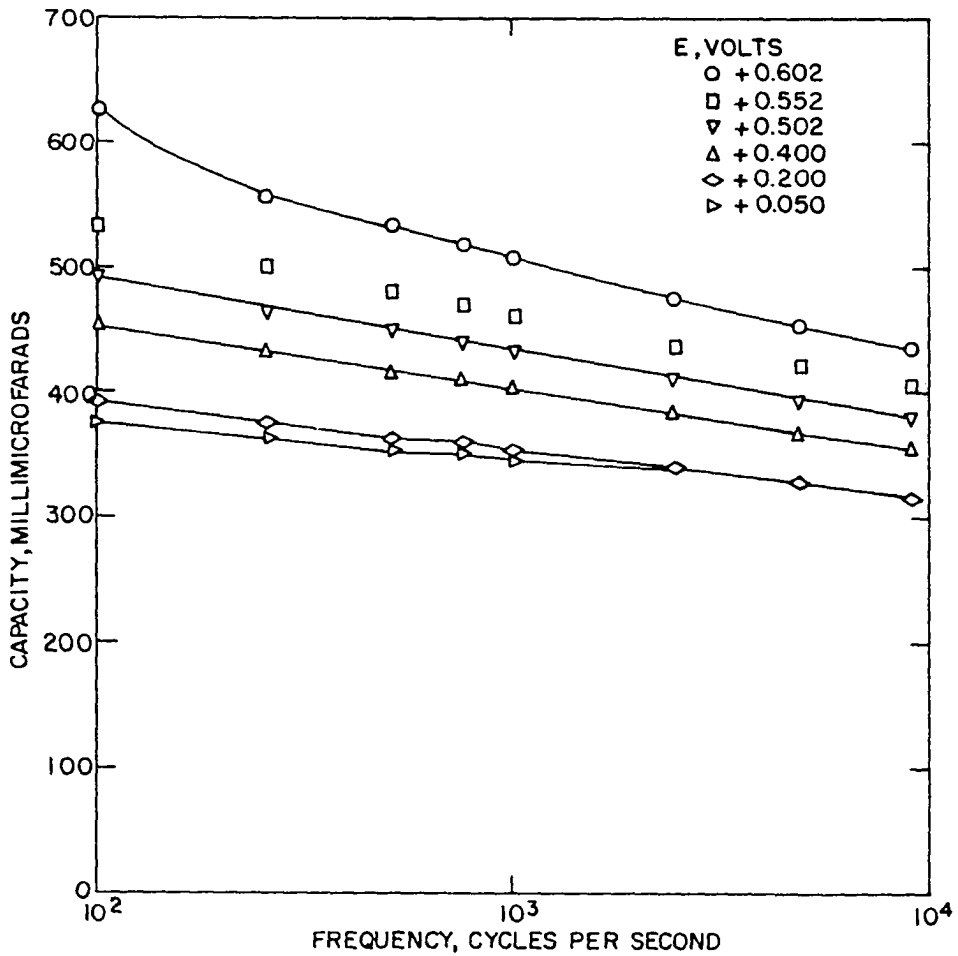
E, VOLTS
+0.602
+0.552
+0.502
+0.400
+0.200
+0.050
700
600
500
400
300
200
100
0
CAPACITY, MILLIMICROFARADS
10^2
10^3
10^4
FREQUENCY, CYCLES PER SECOND

Figure 9. Frequency dependence of capacity of mercury electrode in 1.15 M perchloric acid solution at 54.7°C. Representative polarizations, E, relative to the hydrogen electrode at 54.7°C. Electrode area - 0.01156 cm^2

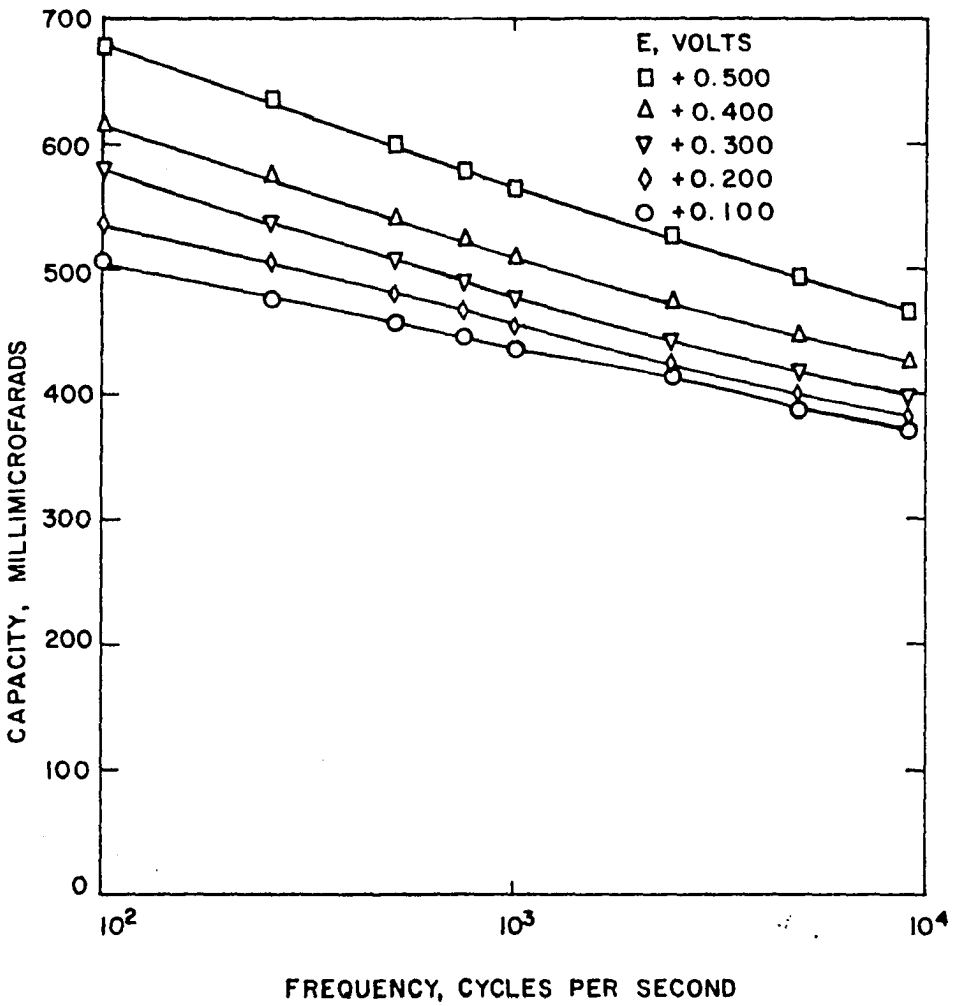
E, VOLTS
+0.500
+0.400
+0.300
+0.200
+0.100
700
600
500
400
300
200
100
0
CAPACITY, MILLIMICROFARADS
10^2
10^3
10^4
FREQUENCY, CYCLES PER SECOND

Figure 10. Frequency dependence of capacity of mercury electrode in 0.05 M potassium perchlorate - 10^{-5} M perchloric acid at 0.5°C. Polarizing potential, E, for representative measurements given with respect to hydrogen electrode at 0.5°C. Electrode area - 0.01156 cm^2

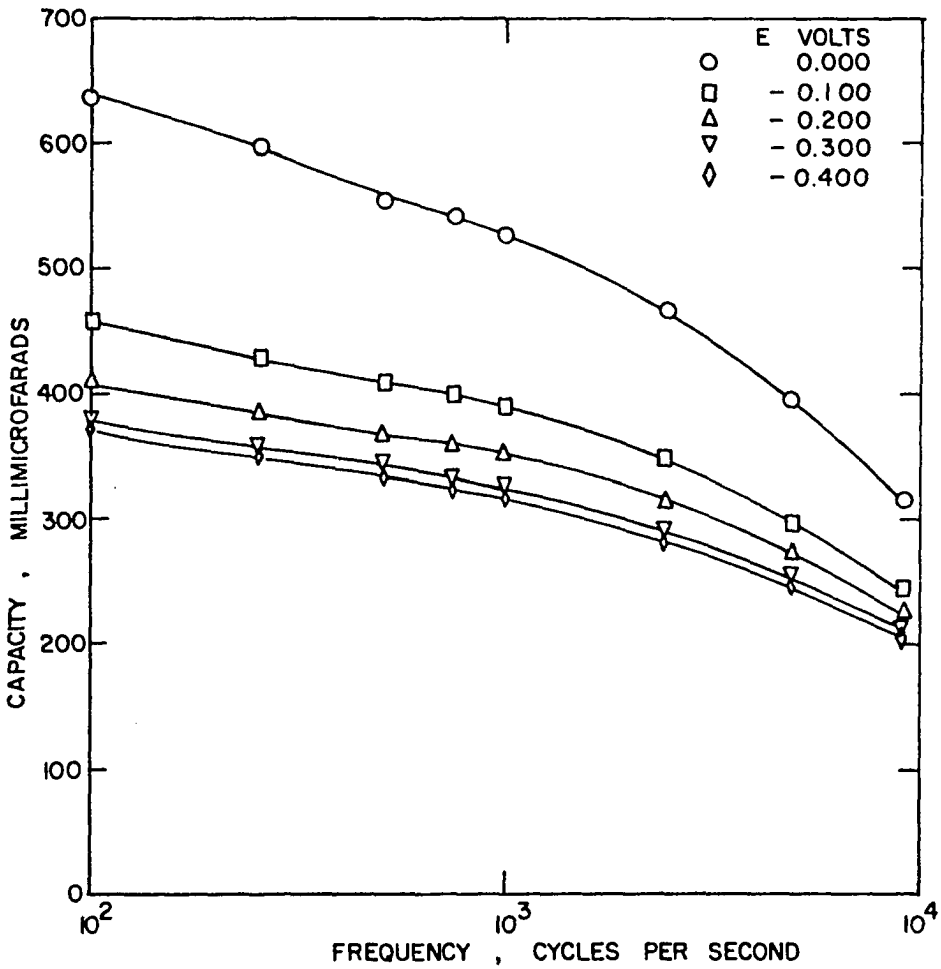
E VOLTS
0.000
- 0.100
- 0.200
- 0.300
- 0.400
700
600
500
400
300
200
100
0
CAPACITY , MILLIMICROFARADS
10^2
10^3
10^4
FREQUENCY , CYCLES PER SECOND

Figure 11. Capacity as function of frequency for mercury-aqueous interface formed in 0.05 M $HClO_4$ - 10^{-5} M $HClO_4$ at 25°C, shown for several polarizing potentials, E, relative to the hydrogen electrode. Electrode area - 0.01156 cm^2

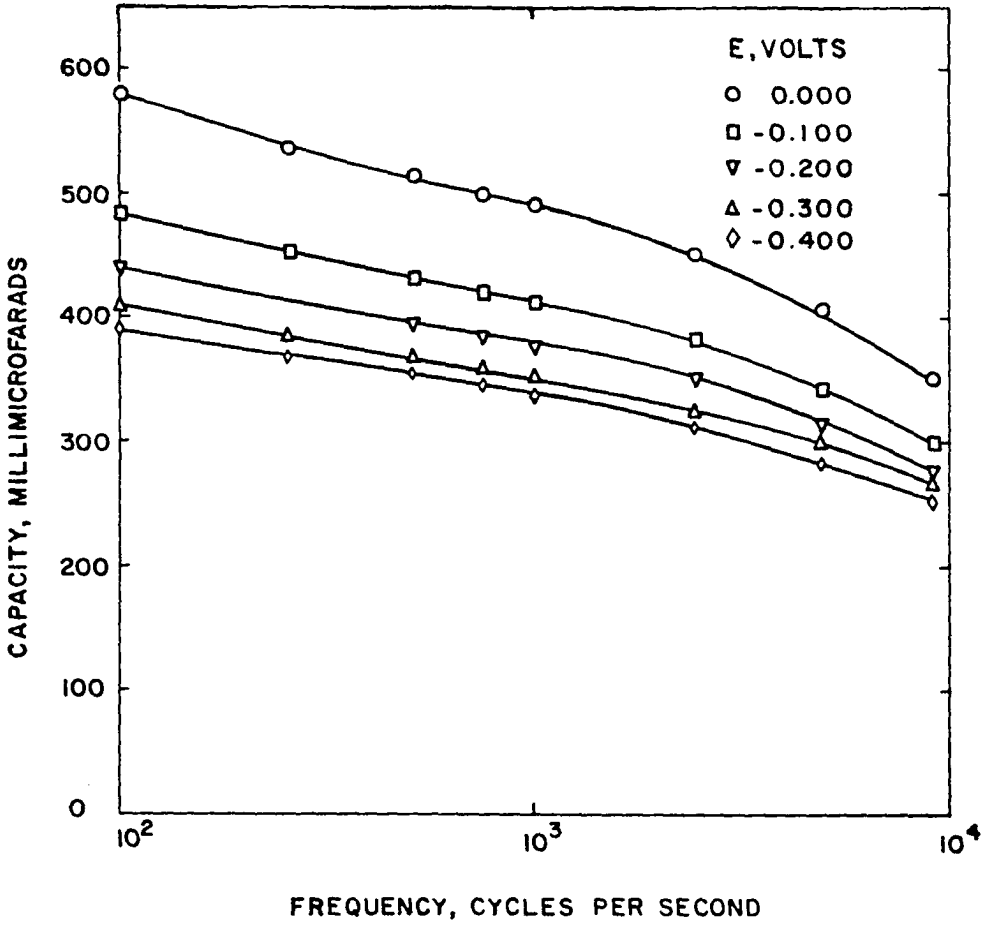
E, VOLTS
0.000
-0.100
-0.200
-0.300
-0.400
600
500
400
300
200
100
0
10^2
10^3
10^4
CAPACITY, MILLIMICROFARADS
FREQUENCY, CYCLES PER SECOND

Figure 12. Capacity of mercury electrode as a function of frequency for 0.05 M potassium perchlorate-10^{-5} M perchloric acid at 54.7°C. Polarizing potential, E, in volts with respect to hydrogen electrode. Electrode area - 0.01156 cm^2

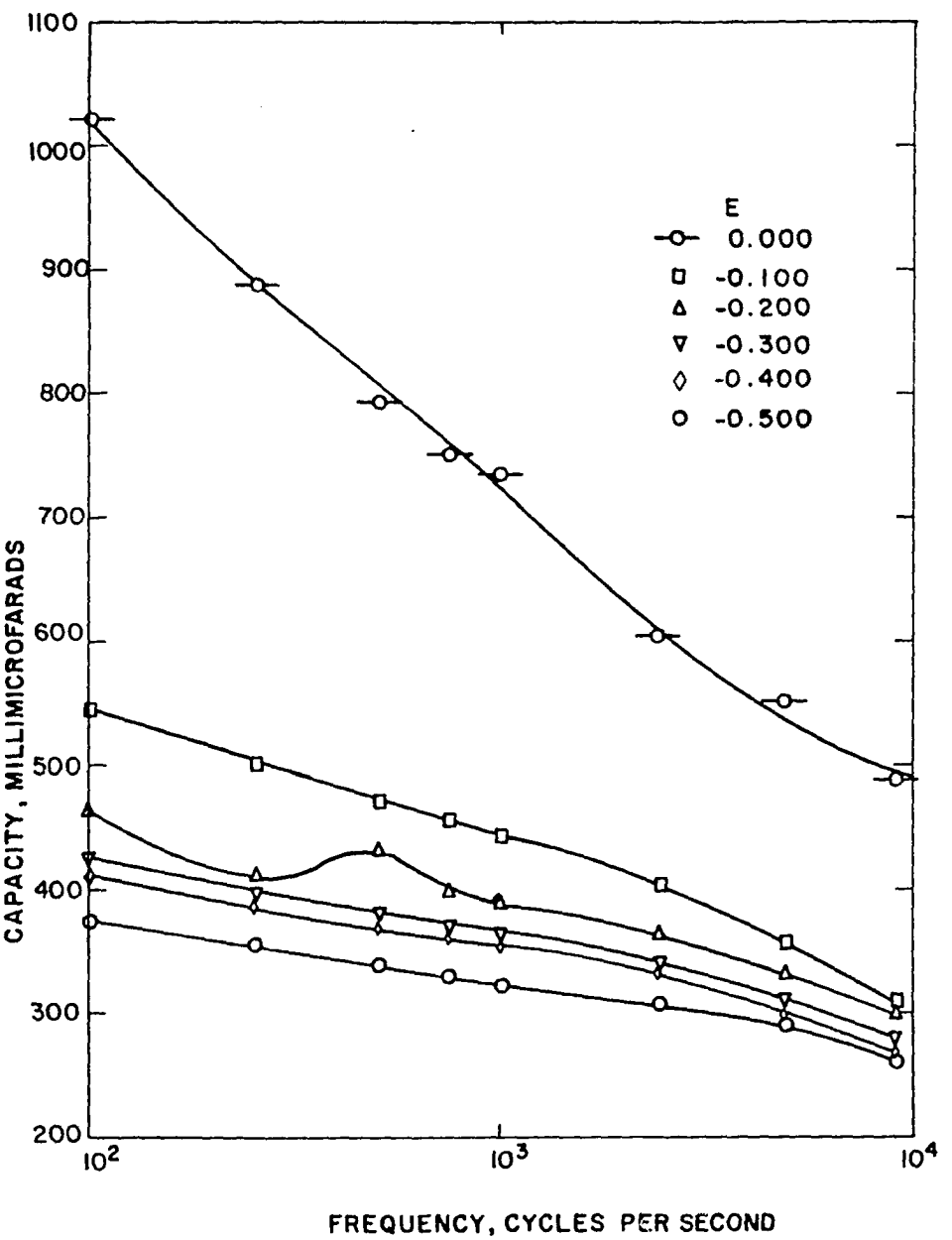
1100
1000
900
800
700
600
500
400
300
200
10^2
10^3
10^4
CAPACITY, MILLIMICROFARADS
FREQUENCY, CYCLES PER SECOND
E
0.000
-0.100
-0.200
-0.300
-0.400
-0.500

Figure 13. Resistance of cell as a function of frequency for mercury electrode in 1.15 M $HClO_4$ at 0.5°C. Polarizing potential, E, referred to hydrogen electrode. Electrode area - 0.01156 cm^2

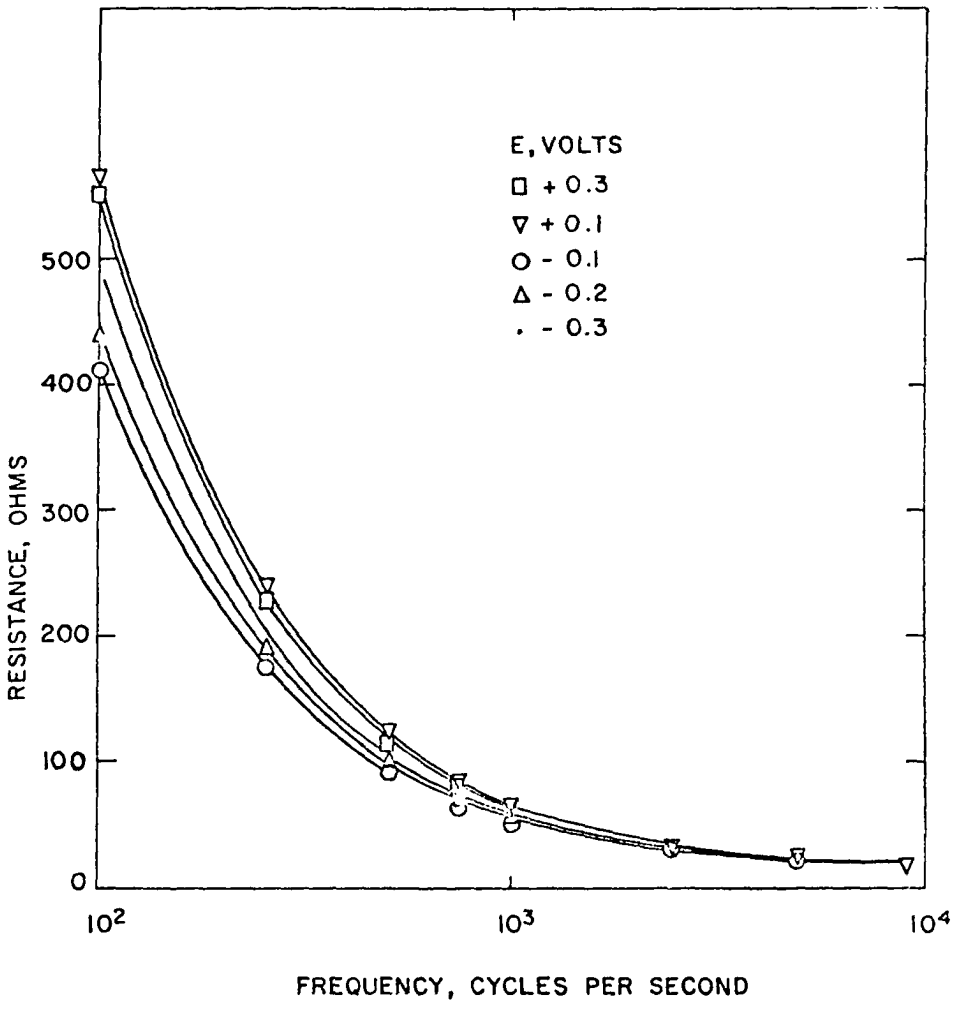
E, VOLTS
□ + 0.3
▽ + 0.1
○ - 0.1
△ - 0.2
• - 0.3
500
400
300
200
100
0
RESISTANCE, OHMS
10²
10³
10⁴
FREQUENCY, CYCLES PER SECOND

Figure 14. Resistance variation with frequency for mercury electrode in 1.15 M $HClO_4$ at 25°C. E, the polarization, given relative to hydrogen electrode. Area of electrode - 0.01156 cm^2

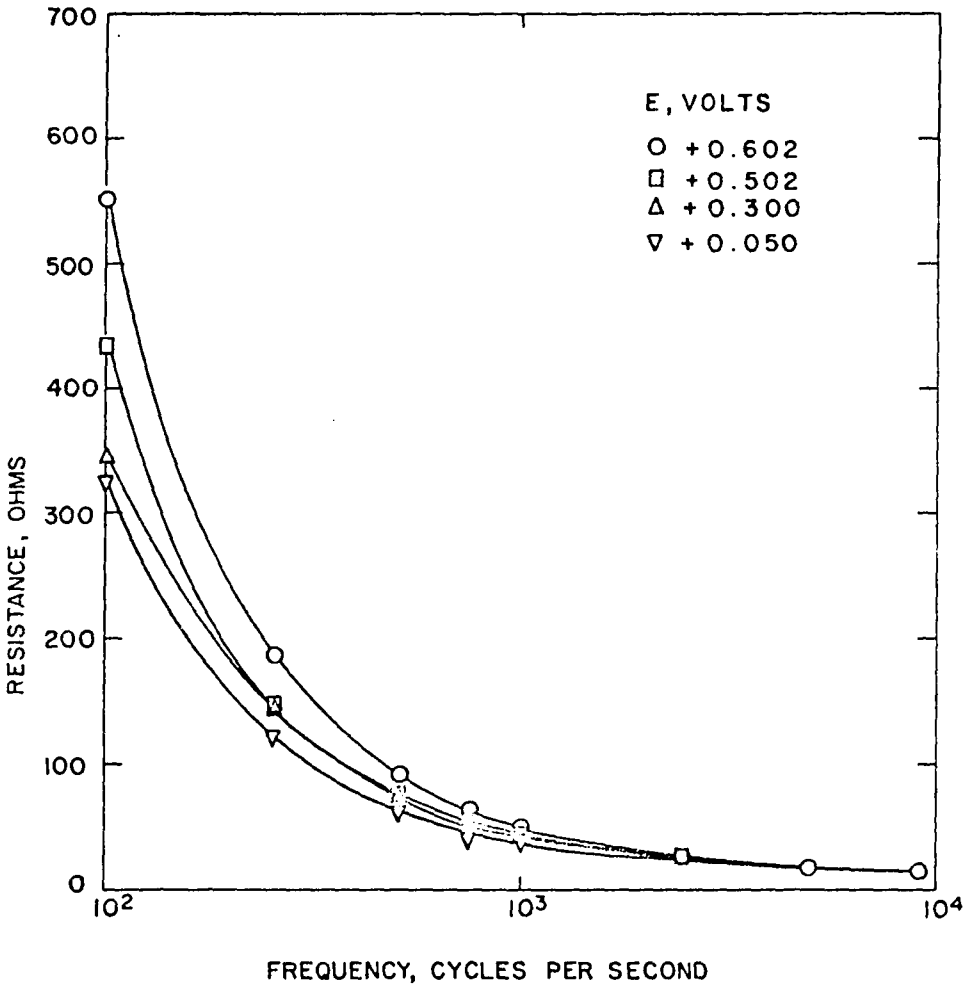
700
600
500
400
300
200
100
0
RESISTANCE, OHMS
E, VOLTS
O +0.602
□ +0.502
Δ +0.300
∇ +0.050
10²
10³
10⁴
FREQUENCY, CYCLES PER SECOND

Figure 15. Cell resistance as a function of frequency for mercury electrode in 1.15 M $HClO_4$ at 54.7°C. Polarization potential, E, given relative to hydrogen electrode. Electrode area - 0.01156 cm^2

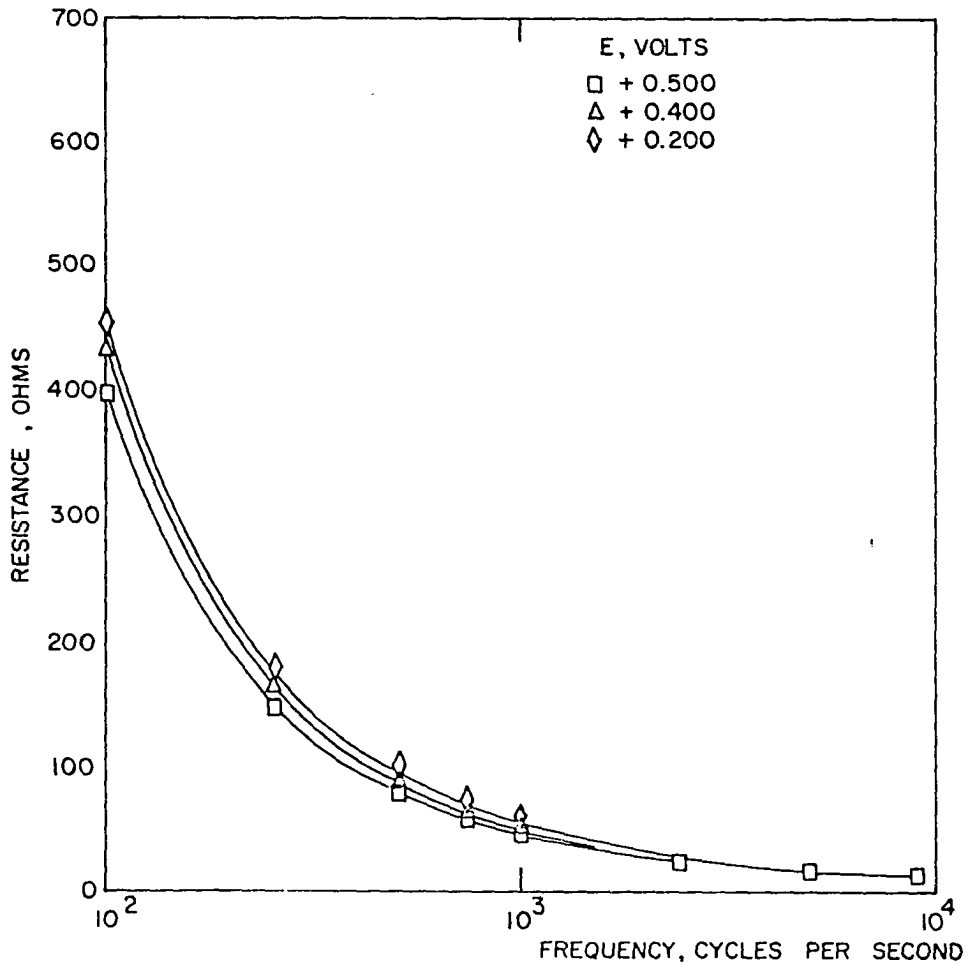
E, VOLTS
□ + 0.500
△ + 0.400
◊ + 0.200
700
600
500
400
300
200
100
0
RESISTANCE , OHMS
10 2
10 3
10 4
FREQUENCY, CYCLES PER SECOND

Figure 16. Frequency dependence of resistance of cell containing 0.05 M potassium perchlorate - 10^{-5} M perchloric acid solution at 0.5°C. Area of mercury electrode - 0.01156 cm^2. E, the polarizing potential, given with respect to hydrogen electrode

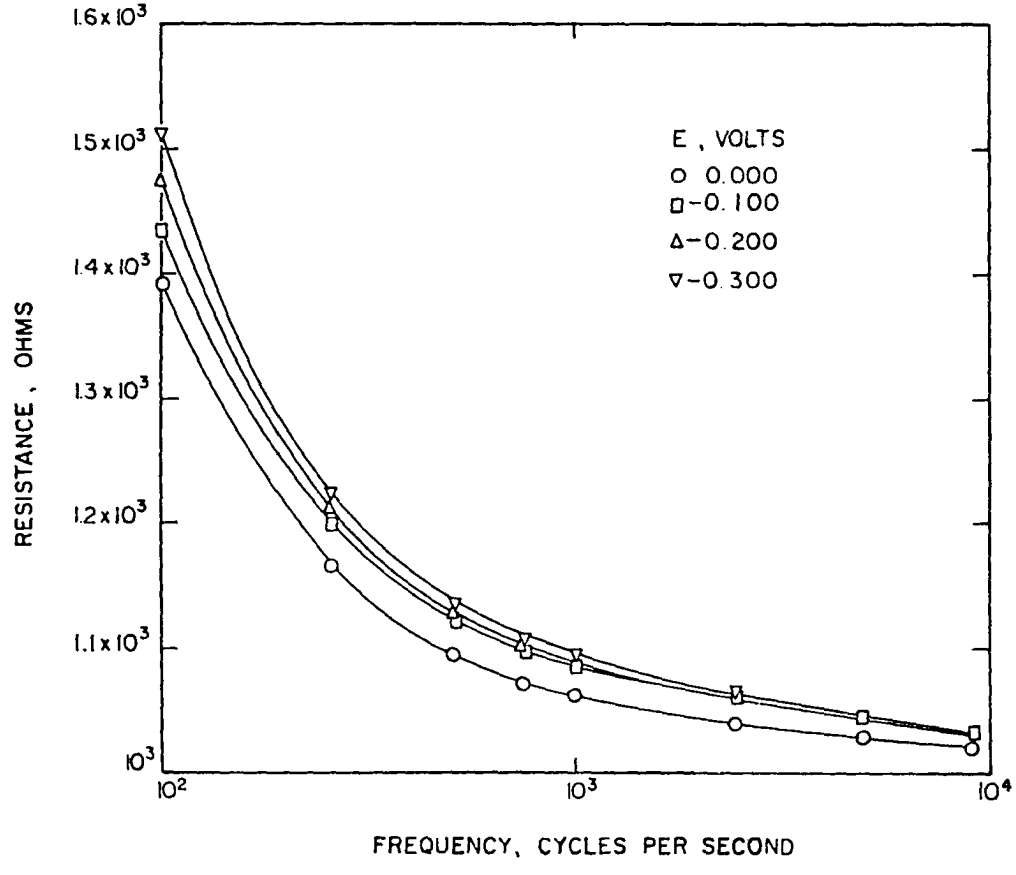
1.6x10³
1.5x10³
1.4x10³
1.3x10³
1.2x10³
1.1x10³
10³
RESISTANCE, OHMS
E, VOLTS
o 0.000
□-0.100
Δ-0.200
▽-0.300
10²
10³
10⁴
FREQUENCY, CYCLES PER SECOND

Figure 17. Cell resistance as function of frequency for mercury electrode in 0.05 M $KClO_4$ - 10^{-5} M $HClO_4$ at 25°C. Polarizing potential, E, referred to hydrogen electrode. Mercury electrode area - 0.01156 cm^2

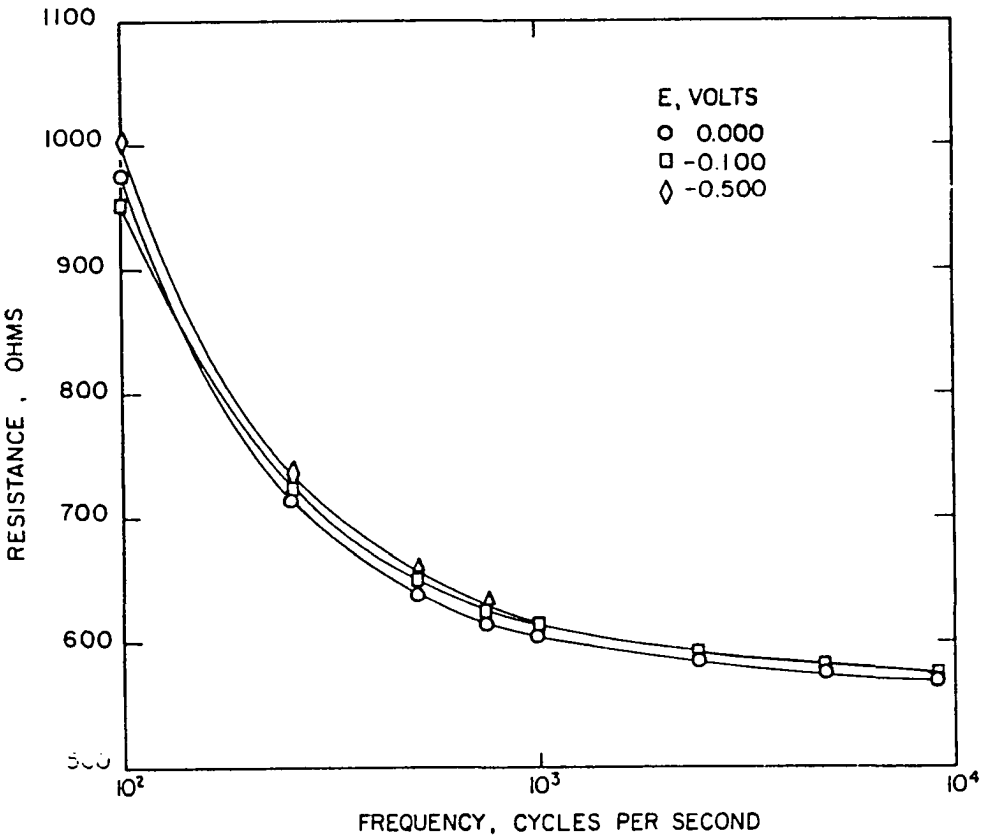
1100
1000
900
800
700
600
500
RESISTANCE , OHMS
E, VOLTS
o 0.000
□ -0.100
◊ -0.500
10^2
10^3
10^4
FREQUENCY, CYCLES PER SECOND

Figure 18. Resistance variation of cell with frequency for mercury electrode in 0.05 M $KClO_4$ - 10^{-5} $HClO_4$ at 54.7°C. Mercury polarizing potential, E, relative to hydrogen electrode. Area of mercury electrode - 0.01156 cm^2

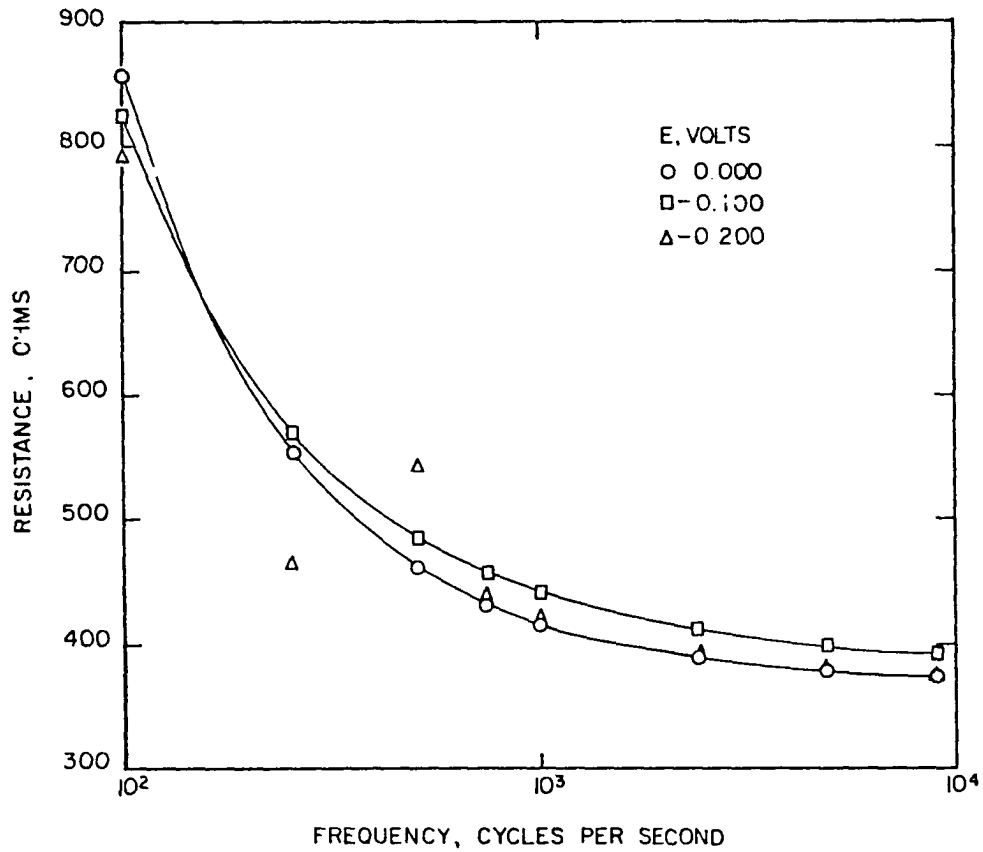
900
800
700
600
500
400
300
RESISTANCE, OHMS
E, VOLTS
O 0.000
□ - 0.100
Δ - 0.200
10²
10³
10⁴
FREQUENCY, CYCLES PER SECOND

The symbols used have the following significance:

ϵ_∞ = dielectric constant for very high frequencies;

ϵ_0 = low frequency or constant field dielectric constant;

ω = angular frequency of the field or 2π/Period;

τ = relaxation time.

Others, notable among whom is Fröhlich (26), have adopted somewhat less mechanistic and more formal approaches to this problem. A time dependent function is assumed to describe the displacement when a field is applied to the dielectric. A superposition principle is applied and the displacement is found to follow

$$D(t) = \epsilon_\infty E(t) + \int_0^t E(u)\alpha(t-u)du \qquad (15)$$

when

$D(t)$ = time dependent displacement,

$E(t)$ = time dependent applied field,

$\alpha(t)$ = a decay function describing the return of the displacement to zero when a steady field is removed.

When the field is periodic and one uses the relation $D(t) = \epsilon E(t)$, there result equations similar in form to the Debye equations but with the quantity

$$\left(\frac{\epsilon_0 + 2}{\epsilon_\infty + 2}\right)\tau$$

in Debye's results replacedby τ in Fröhlich's results. In

either case, the use of the complex dielectric constant permits use of Ohm's law for alternating currents to predict the frequency response of a condenser filled with a dielectric material having a relaxation time. Comparison with an equivalent impedance in the form of a parallel combination of a resistor, R, and a condenser, C, filled with a dielectric having zero relaxation time leads to expressions for the real and imaginary parts of the dielectric constant in terms of R and C. Thus,

$$\epsilon' = \frac{C}{C_o} \text{ and } \epsilon'' = \frac{1}{\omega R C_o} \tag{16}$$

where C_o is the capacity of the empty condenser and $C\epsilon$ is its complex capacity when filled.

If the relaxation in a dielectric is not the simple rotational Brownian motion with a single inner friction constant as assumed by Debye, the frequency dependence of the dielectric constant may sometimes be treated as due to several independent relaxation phenomena each with a time constant τ_k and a characteristic constant $\Delta\epsilon_k$ analogous to $\epsilon_o - \epsilon_\infty$ for the single relaxation mode. Then

$$\epsilon = \epsilon_\infty + \sum_{k=1}^{n} \frac{\Delta\epsilon_k}{1 + i\omega\tau_k} \tag{17}$$

with the real part given by

$$\epsilon' = \epsilon_\infty + \sum_{k=1}^{n} \frac{\Delta\epsilon_k}{1 + \omega^2\tau_k^2} \tag{18}$$

and the imaginary part by

$$\epsilon'' = \sum_{k=1}^{n} \frac{\Delta\epsilon_k \tau_k}{1 + \omega^2\tau_k^2} \tag{19}$$

Other dielectrics may be characterized not by a set of discrete relaxation times but by a distribution function, $f(\tau)$, in which case the complex dielectric constant is given by

$$\epsilon(\omega) = \epsilon_\infty + \int_0^\infty \frac{f(\tau)d\tau}{1 + i\omega\tau} \tag{20}$$

The application of any of these ideas is often difficult, requiring accurate frequency dependence data over a wide frequency range centered about $\omega_{0k} = 1/\tau_k$.

The existence of discrete orientations of dipoles has been postulated, especially for solids, and the ideas of chemical kinetics and absolute reaction theory have been applied (27).

Kurosaki (28) measured the dielectric constant of silica gel as a function of frequency for increasing amounts of adsorbed water vapor. He found a frequency dependence which could be characterized by a relaxation time of about 10^{-5} second. The relaxation time was a function of coverage and became somewhat smaller as the coverage increased. There seemed to be a trend toward some limit in the imaginary part of the dielectric constant. The dielectric constant increased as coverage increased and seemed to show an abrupt change in slope of the curve ϵ' vs. water content in two places.

Kurosaki interpreted this as due to a transition to bulk water properties as the coverage increased. The discrepancy between his value for the relaxation time of water in the surface phase and that of bulk water could be explained by the tight bonding between silica gel and water. A higher activation energy for rotating a surface dipole would thus be expected and should lead to a larger relaxation time.

Zimmerman et al. (29) studied water vapor adsorbed on silica gel using nuclear magnetic resonance techniques. The polyphase character of adsorbed water was considered by them to be demonstrated by the appearance of two distinct relaxation times. They consider that the relaxation times from NMR techniques are of the same order of magnitude as the dielectric relaxation times and, thus, qualitatively verify the results of Kurosaki.

With this background it is easy to imagine that the water molecules in the electrical double layer might possess kinetic properties quite different from those of bulk water. It is logical to expect that a frequency dependence observed for the double layer capacity and resistance could be explained by proper choice of relaxation times and other parameters.

Hansen and Hickson (30) were able to explain their capacity and resistance data for mercury in perchloric acid solution by the proper choice of two relaxation times. Bockris and Conway (21) could represent the frequency dependence of

their resistance and capacity data for copper in sulfuric acid solution in terms of a distribution of relaxation times peaked at about 10^{-6} second. Grantham (22) used two relaxation times somewhat larger than those of Hansen and Hickson to explain the results of measurements of capacity and resistance as functions of frequency for mercury in perchloric acid solutions.

The difficulties in explaining the observed frequency dependences reported by the above authors stemmed largely from a lack of precision in the resistance measurements. The choice of electrode III was dictated mainly by this consideration. Measurements of resistance and capacity could be duplicated to within 0.5 per cent when the mercury surface was renewed. The capacity was quite stable over a half-hour period and, though the measurements gave somewhat larger capacity values than Grahame (10) reported, it was believed that the results of measurements on this electrode were more likely to be amenable to a theoretical treatment than on dropping mercury electrodes or pendant mercury drops. An additional advantage lay in the reproducible area resulting after each surface renewal. Only one area determination was necessary in the entire series of measurements as contrasted to one determination for each measurement with the dropping mercury electrode.

Since the capacity and resistance values presented in Tables 1 - 12 are the series equivalent to the cell, it was

necessary to convert to a parallel equivalent for the double layer to test the dielectric relaxation theory. This was accomplished by extrapolation of plots of resistance versus reciprocal frequency to infinite frequency. This extrapolated resistance was attributed to the solution and all cell resistances were diminished by this quantity to arrive at the resistance due to the electrode interface. The series capacity and resistance of the double layer were converted to the complex dielectric constant multiplied by a constant C_0, which can be regarded as the capacity of the double layer region if only point charges were present and the dielectric constant were unity. The relations used were

$$C_0\epsilon' = \frac{C}{1 + \omega^2 R^2 C^2} \tag{21}$$

and

$$C_0\epsilon'' = \frac{\omega R C^2}{1 + \omega^2 R^2 C^2} \tag{22}$$

Representative values are tabulated in Table 13 and 14 and $C_0\epsilon'$ and $C_0\epsilon''$ are displayed as functions of frequency in Figures 19 and 20. A plot of a theoretical $C_0\epsilon'$ and $C_0\epsilon''$ for hypothetical values of τ, $C_0\Delta\epsilon$, and $C_0\epsilon_\infty$ is compared with the curves calculated from the experimental quantities. The agreement is hardly satisfactory in either case. Attempts to find a distribution function for relaxation times were equally unsuccessful in explaining these data.

Table 13. Apparent $C_0\epsilon'$ values calculated from experimental data in 1.15 M $HClO_4$ for several signal frequencies and several polarizations at 25°C[a]

E	Frequency								R_∞ [b]
	100	255	505	754	997	2425	4890	9060	
0.000	370	358	348	348	342	332	324	316	10.90
+0.100	360	347	338	337	331	322	314	305	11.15
+0.200	389	373	361	359	338	351	327	317	10.00
+0.300	410	393	382	380	371	355	343	332	10.80
+0.400	444	427	412	408	398	379	364	353	11.10
+0.502	485	462	446	440	431	409	392	377	10.45

[a]Polarizing potential, E, in volts relative to a hydrogen electrode at 25°C. $C_0\epsilon'$ in millimicrofarads. Frequency in cycles per second.

[b]R_∞ extrapolated from cell resistance values.

Table 14. Apparent $C_o\epsilon''$ values calculated from experimental data in 1.15 M $HClO_4$ for several signal frequencies and several polarizations at 25°C[a]

E	Frequency								R_∞ [b]
	100	255	505	754	997	2425	4890	9060	
0.000	32.2	23.9	20.9	16.7	18.7	20.7	18.8	18.6	10.90
+0.100	30.9	23.1	24.5	17.8	18.6	18.2	18.0	16.8	11.15
+0.200	37.1	27.8	27.1	21.4	24.2	24.6	24.5	23.6	10.00
+0.300	35.7	33.6	30.5	25.7	28.0	27.3	26.5	24.6	10.80
+0.400	59.3	42.4	36.9	32.3	34.4	31.9	29.0	24.7	11.10
+0.502	64.3	47.6	41.7	35.9	39.7	37.1	35.2	32.5	10.45

[a]Polarizing potential, E, in volts relative to a hydrogen electrode at 25°C. $C_o\epsilon''$ in millimicrofarads. Frequency in cycles per second.

[b]R_∞ extrapolated from cell resistance values.

Figure 19. Frequency dependence of capacity, as apparent $C_o\epsilon'$, compared to the frequency dependence of $C_o\epsilon'$ for a hypothetical dielectric. Points calculated from experimental data taken at 25°C in 1.15 M $HClO_4$ with a mercury electrode area of 0.01156 cm^2. Results given for several polarizing potentials, E. Curve computed for relaxation time, $\tau = 1.57 \times 10^{-3}$ seconds, $C_o\Delta\epsilon = 130$ millimicrofarads and $C_o\epsilon_\infty = 350$ millimicrofarads

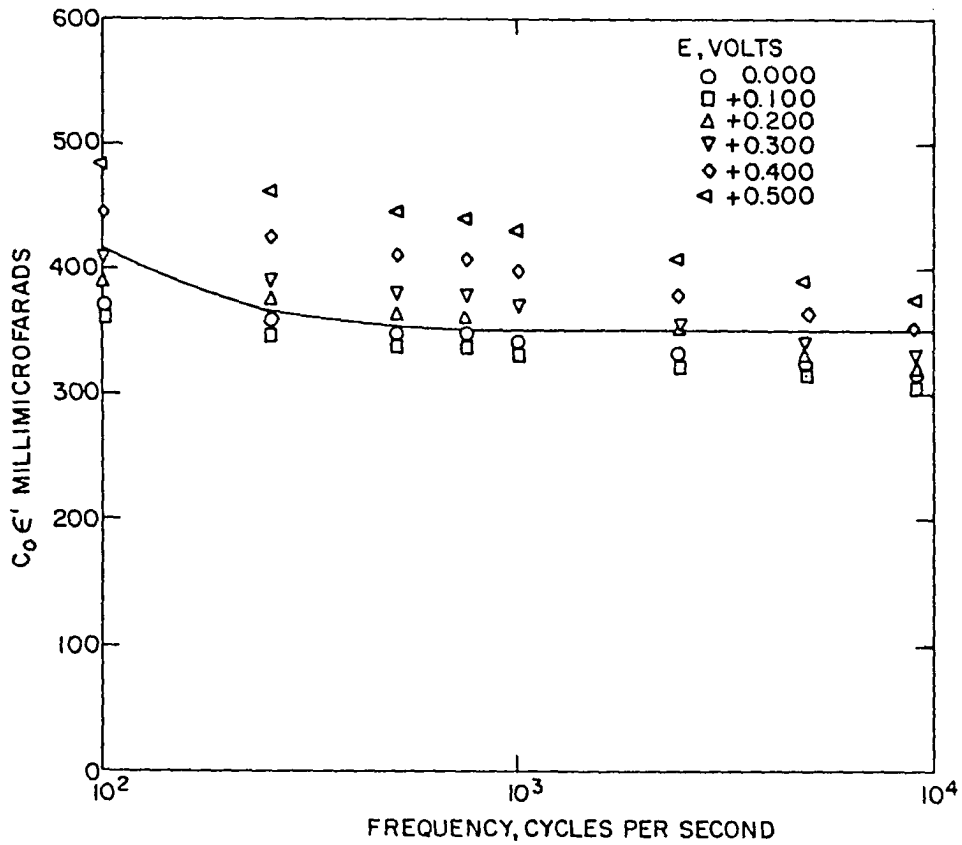
E, VOLTS
0.000
+0.100
+0.200
+0.300
+0.400
+0.500
600
500
400
300
200
100
0
$C_0\epsilon'$ MILLIMICROFARADS
10^2
10^3
10^4
FREQUENCY, CYCLES PER SECOND

Figure 20. Apparent $C_o\epsilon''$ as function of frequency compared to $C_o\epsilon''$ for a hypothetical dielectric. Points calculated from experimental data taken at 25°C in 1.15 M $HClO_4$ with a mercury electrode area of 0.01156 cm^2. Results for several polarization potentials, E, are shown. Curve computed for relaxation time, $\tau = 1.57 \times 10^{-3}$ seconds and $C_o\Delta\epsilon$ = 130 millimicrofarads

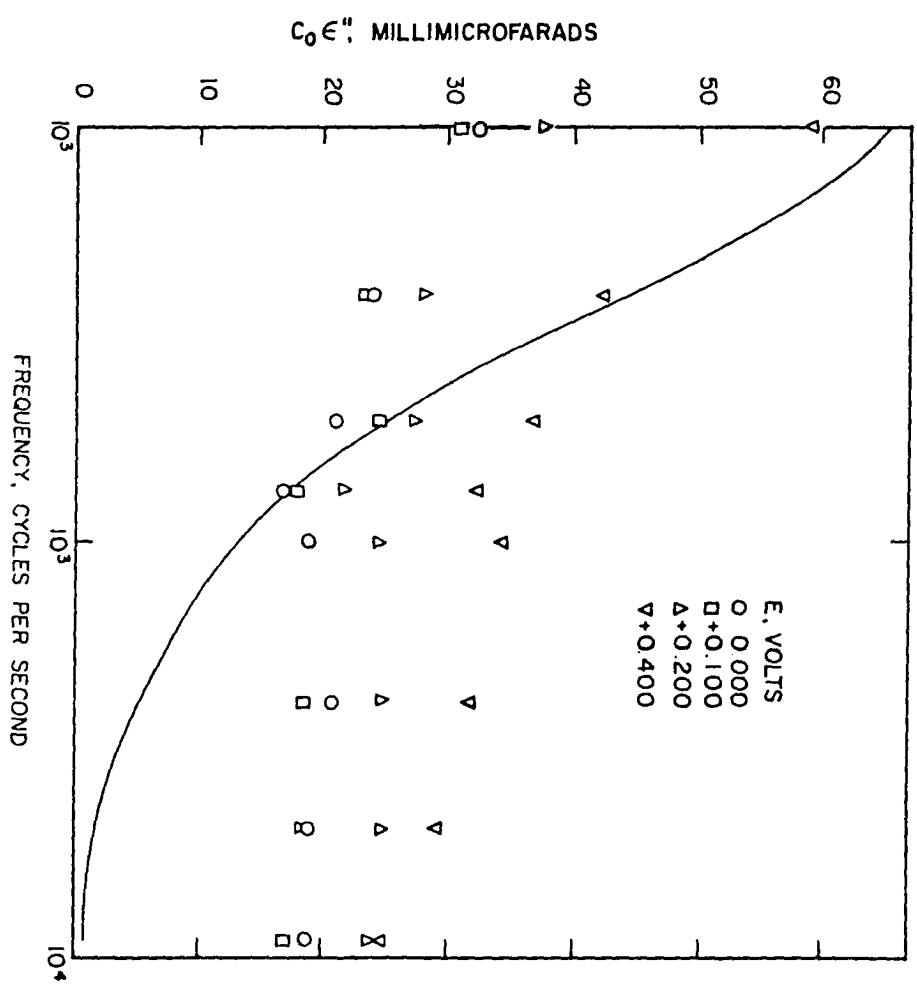
$C_0\epsilon''$, MILLIMICROFARADS
0
10
20
30
40
50
60
10^3
10^3
10^4
FREQUENCY, CYCLES PER SECOND
E, VOLTS
○ 0.000
□ +0.100
△ +0.200
▽ +0.400

In every attempt to explain $C_0\epsilon'$ and $C_0\epsilon''$ in terms of the parameters $C_0(\epsilon_0 - \epsilon_\infty)$, $C_0\epsilon_\infty$ and τ, or the analogous parameters which characterize systems with more than one relaxation time, fairly good representations for either $C_0\epsilon'$ or $C_0\epsilon''$ could be obtained but never for both quantities. The experimental data were generally tested by choosing parameters which best represented $C_0\epsilon''$ and comparing the function $C_0\epsilon'$ calculated from these parameters according to the particular model assumed with the experimental value. The discrepancy between the calculated function $C_0\epsilon'$ and the observed values was far greater than experimental error. Further, it can be shown (26) that, if an arbitrary function $\alpha(x)$ can be used to generate ϵ' and ϵ'' according to

$$\epsilon'(\omega) - \epsilon_\infty = \int_0^\infty \alpha(x) \cos \omega x \, dx$$

and

$$\epsilon'' = \int_0^\infty \alpha(x) \sin \alpha x \, dx,$$

then

$$\epsilon'(\omega) - \epsilon_\infty = \frac{2}{\pi} \int_0^\infty \epsilon''(u) \frac{u}{u^2 - \omega^2} \, du \qquad (23)$$

and

$$\epsilon''(\omega) = \frac{2}{\pi} \int_0^\infty \left[\epsilon'(u) - \epsilon_\infty \right] \frac{\omega}{\omega^2 - u^2} \, du.$$

Investigation of the frequency dependence of ϵ' and ϵ'' was

limited to the range $10^2 < f < 10^4$ cycles per second, so numerical evaluation of the integral in Equation 23 involved extrapolation of experimental results. For what appeared a reasonable range of extrapolations, however, results obtained were not in accord with Equation 23. It, therefore, does not seem likely that dielectric relaxation can account for the observed dispersion of capacitance and resistance.

Other likely sources of the dispersion were considered before the final explanation was found. Since, according to Equation 1, the surface tension of mercury is potential dependent, application of a small sinusoidal variation of the potential about a constant value should result in oscillations of the mercury surface about its mean position. Thus, periodic variations of the surface area should arise and consequent variations in capacity should be evident. Such behavior should be frequency dependent as well as amplitude dependent. However, no measureable changes in capacity could be observed for either flat surfaces or spherical ones for amplitudes of periodic voltages less than 100 millivolts. At potentials somewhat higher, the onset of standing wave formation on both the flat mercury surface and the spherical surface could be observed with a microscope for low frequencies. The signals used in the measurements reported here were always less than 5 millivolts so this effect would not be reflected in these results.

Since gold does not form a bond with glass as tungsten, for example, does, a small separation of the gold tube of the electrode from its glass supporting sheath might be expected. The width of the annulus between glass and gold can be estimated from a knowledge of the thermal expansion coefficients of the two materials and an estimate of a solidification temperature for glass. The manner of sealing the gold tube in the glass capillary insures that a one atmosphere pressure differential is exerted on the walls of the glass tending to collapse the glass onto the gold. The annealing temperature of Pyrex is usually given as 550°C. If this temperature is taken as that below which flow of the Pyrex does not occur under application of pressure, the width of the annulus w is given by

$$w = (T_1 - T_2)(\ell_1 - \ell_2)r \qquad (24)$$

where T_1 is the solidification temperature, T_2 is room temperature, ℓ_1 is the thermal coefficient of expansion for gold and ℓ_2 is that for Pyrex, and r is the radius of the gold tube. With the following values (31)

$$T_1 = 550°C$$
$$T_2 = 25°C$$
$$\ell_1 = 14.2 \times 10^{-6}\ \text{deg}^{-1}$$
$$\ell_2 = 3.2 \times 10^{-6}\ \text{deg}^{-1}$$
$$r = 0.06\ \text{cm.}$$

there results the value 3.47×10^{-4} cm.

The effect of solution penetrating this annulus must be considered. At first glance it might appear that no effect could arise here. It might be argued that the conductivity of the mercury is so great that the solution in the annulus is effectively short circuited by the mercury column. That this is not the case can be demonstrated by the following argument.

Due to the high conductivity of the mercury and the small currents flowing in the circuit, the entire mercury surface is very nearly an equi-potential surface. This fact implies that the capacity per unit area is uniform over all the mercury surface in contact with the solution. Thus, the mercury wetting the gold along the annular wall has the same capacity per unit area as the flat mercury surface at the end of the tube. If alternating current crosses the annular wall and flows through the solution in the annulus, each element of area along the gold tube has the same capacity per unit area but a different resistance which increases as the element is chosen farther from the end of the tube. The equivalent circuits shown in Figure 21 approximate the entire cell impedance. Part (a) shows the regions in the electrode surrounding the annulus. Part (b) shows the annular equivalent as an open ended transmission line with uniform resistance per unit length and uniform capacity per unit length. Parts (c), (d), and (e) show the transmission line connected in parallel with the series equivalent to the solution resistance and capacity at

Figure 21. Circuit elements equivalent to the cell impedance according to a distributed capacity or transmission line hypothesis

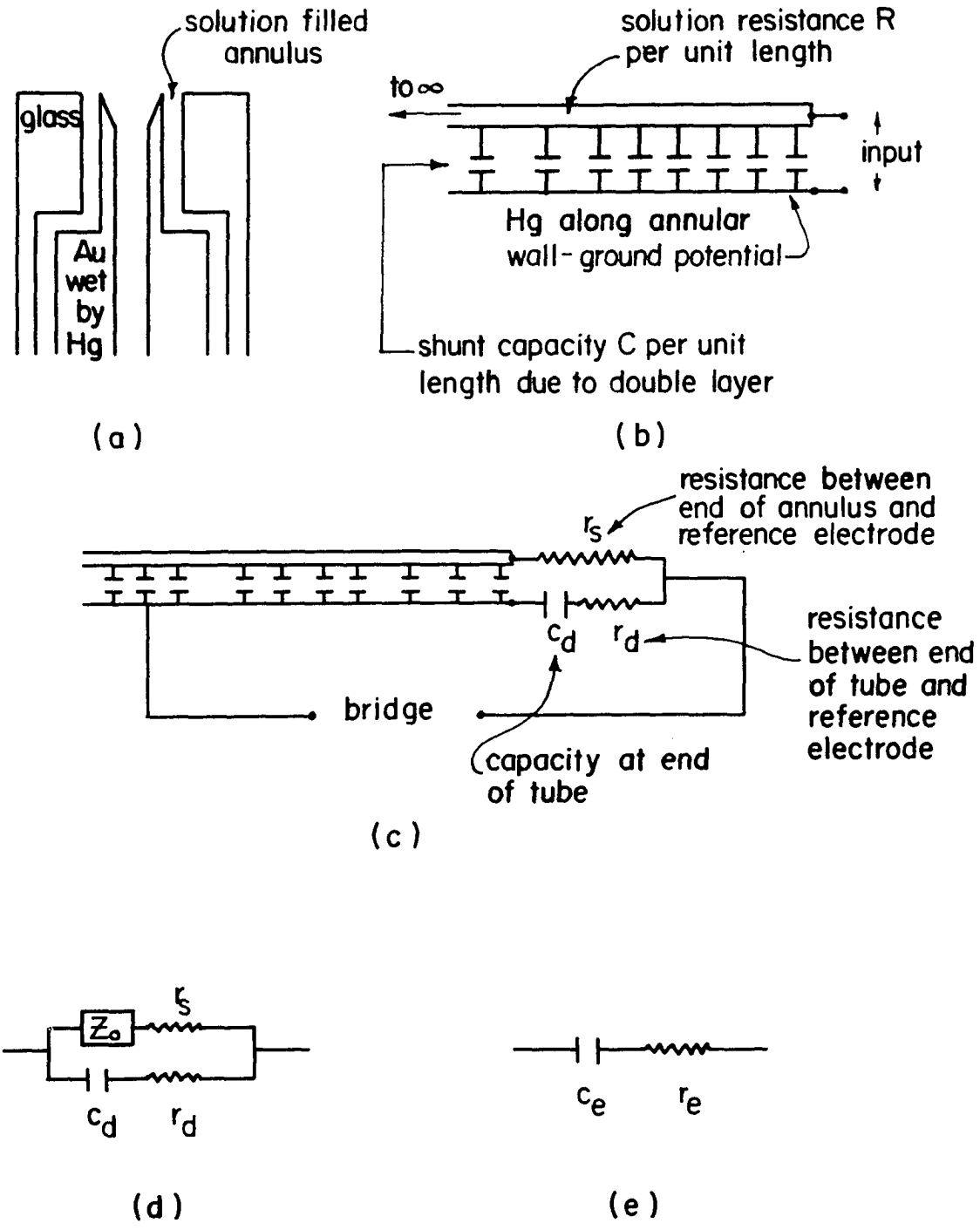
solution filled annulus
glass
Au wet by Hg
(a)
solution resistance R per unit length
to ∞
input
Hg along annular wall - ground potential
shunt capacity C per unit length due to double layer
(b)
resistance between end of annulus and reference electrode
r_s
c_d
r_d
resistance between end of tube and reference electrode
bridge
capacity at end of tube
(c)
r_s
Z_o
c_d
r_d
(d)
c_e
r_e
(e)

the flat mercury surface at the end of the tube, a proposed cell equivalent circuit and the experimental equivalent. The estimate of the effect of the annulus must be represented in some way similar to that in part (d) but this is by no means unique.

For the sake of analysis the annulus is assumed to be uniform in width and self induction absent from it. The transmission line equations are then (32, 33)

$$\frac{\partial V}{\partial x} = -IR \tag{25}$$

and

$$\frac{\partial I}{\partial x} = -YV \tag{26}$$

where V is the potential at a point, x, along the annulus, I is the current at the point, R is the resistance per unit length, and Y is the admittance per unit length given in turn by $Y = i\omega C$. The admittance Y provides the current path between the two conductors of the transmission line, the one uniformly at ground potential taken to be the mercury covered gold tube and the other with a uniform resistance and a potential distribution along it taken to be the solution in the annulus. The solutions to this set of equations are

$$V = Ae^{ax} + Be^{-ax} \tag{27}$$

and

$$I = Ge^{ax} + He^{-ax} \tag{28}$$

with $a^2 = RY$ and A, B, G, and H constants to be determined

from the conditions on the equations. From the Equations 25, 27, and 28 we have

$$-R(Ge^{ax} + He^{-ax}) = a(Ae^{ax} - Be^{-ax})$$

whence --

$$G = -\frac{a}{R} A \tag{29}$$

and

$$H = \frac{a}{R} B. \tag{30}$$

Equation 28 may be rewritten as

$$I = -b(Ae^{ax} - Be^{-ax}) \tag{31}$$

where $b^2R^2 = a^2$. Determination of A and B depends on the length of the line assumed and on the terminal load for the line. If the line is infinite in length the terminal conditions are

$$I(\infty) = 0 \tag{32}$$

and

$$V(\infty) = 0. \tag{33}$$

Then, the equations for I and V assume the forms

$$V = Be^{-ax} \tag{34}$$

and

$$I = bBe^{-ax}. \tag{35}$$

At the input end of the line, $V(0) = V_0$ so that

$$B = V_0 \tag{36}$$

and

$$I(0) = bV_0. \tag{37}$$

The impedance of the line can be found from $V_o = I_o Z_o$ and is just $Z_o = b^{-1}$ which in the complex number notation is

$$Z_o = \left(\frac{R}{2C}\right)^{\frac{1}{2}} \frac{1 - i}{\sqrt{\omega}} \tag{38}$$

The equivalent circuit in Figure 21 (d) has an admittance which can be expressed as

$$Z^{-1} = (Z_o + r_s)^{-1} + (r_d + \frac{1}{i\omega C})^{-1} \tag{39}$$

When the expression for Z_o is introduced and the resultant equation is rationalized, one finds for the real and imaginary parts of Z

$$\mathrm{Re}(Z) = \frac{\left[(\omega r_d C_d - 1)\left(\frac{R}{2C}\right)^{\frac{1}{2}} + \omega^{\frac{3}{2}} r_s r_d C_d \right] \left[\omega C_d \left(\frac{R}{2C}\right)^{\frac{1}{2}} + \omega^{\frac{3}{2}} C_d (r_s + r_d) \right]}{\left[\omega C_d \left(\frac{R}{2C}\right)^{\frac{1}{2}} + \omega^{\frac{3}{2}} C_d (r_s + r_d)^2 \right]^2 + \left[\omega C_d \left(\frac{R}{2C}\right)^{\frac{1}{2}} - \sqrt{\omega} \right]^2}$$

$$+ \frac{\left[\omega C_d \left(\frac{R}{2C}\right)^{\frac{1}{2}} - \sqrt{\omega} \right] \left[(\omega r_d C_d - 1)\left(\frac{R}{2C}\right)^{\frac{1}{2}} + r_s \sqrt{\omega} \right]}{\left[\omega C_d \left(\frac{R}{2C}\right)^{\frac{1}{2}} + \omega^{\frac{3}{2}} C_d (r_s + r_d)^2 \right]^2 + \left[\omega C_d \left(\frac{R}{2C}\right)^{\frac{1}{2}} - \sqrt{\omega} \right]^2} \tag{40}$$

$$\mathrm{Im}(Z) = \frac{\left[(\omega r_d C_d - 1)\left(\frac{R}{2C}\right)^{\frac{1}{2}} + r_s \sqrt{\omega} \right] \left[\omega C_d \left(\frac{R}{2C}\right)^{\frac{1}{2}} + \omega^{\frac{3}{2}} C_d (r_s + r_d) \right]}{\left[\omega C_d \left(\frac{R}{2C}\right)^{\frac{1}{2}} + \omega^{\frac{3}{2}} C_d (r_s + r_d)^2 \right]^2 + \left[\omega C_d \left(\frac{R}{2C}\right)^{\frac{1}{2}} - \sqrt{\omega} \right]^2}$$

$$- \frac{\left[\omega C_d \left(\frac{R}{2C}\right)^{\frac{1}{2}} - \sqrt{\omega} \right] \left[(\omega r_d C_d - 1)\left(\frac{R}{2C}\right)^{\frac{1}{2}} + \omega^{\frac{3}{2}} r_s r_d C_d \right]}{\left[\omega C_d \left(\frac{R}{2C}\right)^{\frac{1}{2}} + \omega^{\frac{3}{2}} C_d (r_s + r_d)^2 \right]^2 + \left[\omega C_d \left(\frac{R}{2C}\right)^{\frac{1}{2}} - \sqrt{\omega} \right]^2} \tag{41}$$

Experimentally, Re(Z) is a frequency dependent resistance in series with a frequency dependent capacity. The frequency dependent capacity is related to Im(Z) through the equation

$$(i\omega C_e)^{-1} = -i\ \mathrm{Im}(Z) \tag{42}$$

Due to the complicated dependence of Z on frequency, a check for agreement between theory and experiment based on Equation 40 and 41 is extremely awkward. A somewhat less laborious approach was used to check the validity of the foregoing analysis.

Suppose that the quantities C_e, r_e, C_d, and r_d in Figure 15 (d) and (e) are known. Then $Z_o + r_s$ can be calculated from Equation 39 if $Z = r_e + (i\omega C_e)^{-1}$. This can be done by rearranging Equation 39 to give

$$(Z_o + r_s)^{-1} = (r_e + \frac{1}{i\omega C_e})^{-1} - (r_d + \frac{1}{i\omega C_d})^{-1}. \tag{43}$$

Inverting and rationalizing gives the result

$$\mathrm{Re}(Z_o+r_s) = \frac{C_eC_d(r_e-r_d)(1-\omega^2r_dr_eC_dC_e) + (C_e-C_d)(r_eC_e+r_dC_d)}{\omega^2C_e^2C_d^2(r_e-r_d)^2 + (C_e-C_d)^2} \tag{44}$$

$$\mathrm{Im}(Z_o+r_s) = \frac{(C_e-C_d)(1-\omega^2r_er_dC_eC_d) - \omega^2C_eC_d(r_e-r_d)(r_eC_e+r_dC_d)}{\omega^3C_e^2C_d^2(r_e-r_d)^2 + \omega(C_e-C_d)^2}. \tag{45}$$

Grahame (10) presents in graphical form some data for 1 M perchloric acid solutions at room temperature. C_d was calculated from the known area of the end of the tube and the

capacity per unit area given by Grahame. A value of r_d was estimated based on the extrapolated measurements on the cell.

Figure 22 shows a plot of $Re(Z_o+s)$ derived from Grahame's data and a best curve of $\alpha\omega^{-1/2}$. The agreement between the points calculated for $[\omega\ Im(Z_o+s)]^{-1}$ from Grahame's data and the best curve of $\beta\omega^{-1/2}$ shown in Figure 23 is not so good. The poor agreement might be indicative of an error in the area of the end of the gold arising in edge effects or roughness. Doubtless the capacity per unit area of the mercury-gold amalgam exposed to the solution in the annulus is greater than that of the mercury in the flat interface due to surface irregularities in the gold tube from which the electrode was made. These irregularities in themselves lead to a frequency dependence for the capacity. The results immediately suggest an experiment to verify that apparent frequency dependence of the double layer capacity at mercury-aqueous interfaces is not a property of the double layer. Precision bore capillary tubing of about 5 millimeters outside diameter and 0.062 millimeter internal diameter was heated over a segment two inches in length and, when soft, was pulled to give an extension of about two inches in length. The diameter of the capillary, both inner and outer, decreased as a result. A head of about 40 centimeters of mercury applied to the capillary was necessary to produce a flow rate of 10^{-4} grams per second. A drop of mercury was formed and fell from the tip in sixty to one

Figure 22. Transmission line resistance. Points derived from experimental data. Curve has slope of - 1/2 in accordance with Equation 38

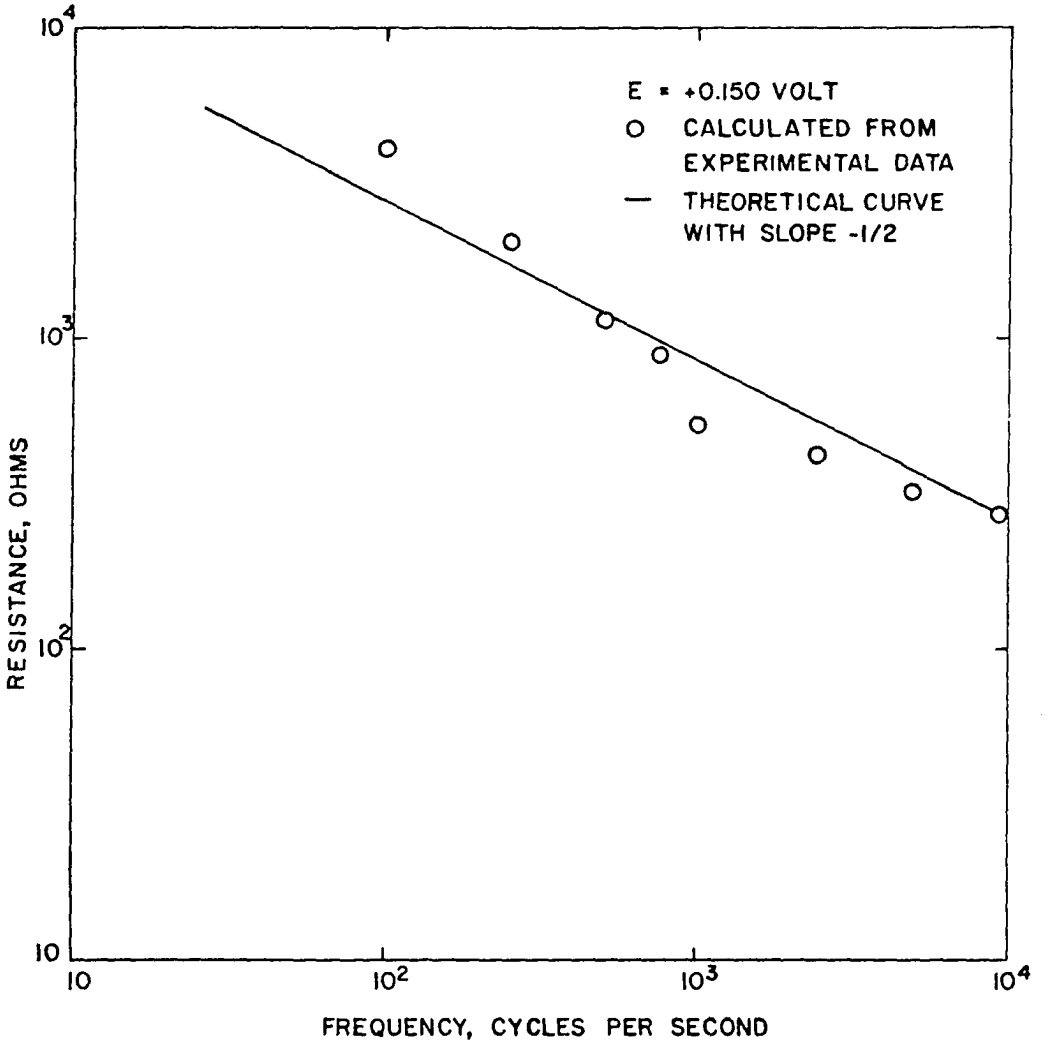
E = +0.150 VOLT
O CALCULATED FROM EXPERIMENTAL DATA
— THEORETICAL CURVE WITH SLOPE -1/2
RESISTANCE, OHMS
FREQUENCY, CYCLES PER SECOND
10
10^2
10^3
10^4

Figure 23. Transmission line capacitance. Points computed from experimental data by means of Equation 44. Curve has slope - 1/2 in accordance with Equation 38

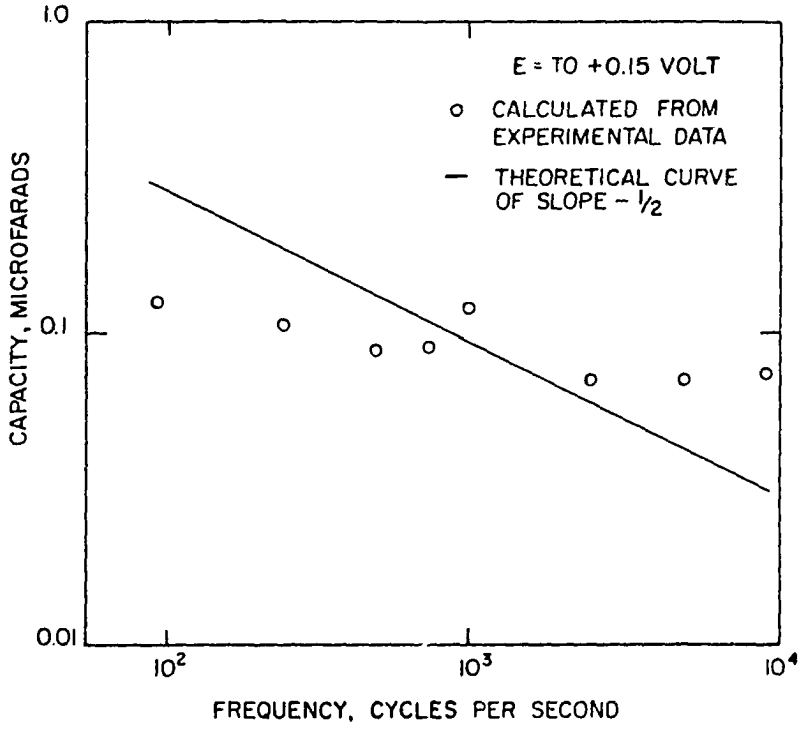
1.0
0.1
0.01
CAPACITY, MICROFARADS
E = TO +0.15 VOLT
CALCULATED FROM EXPERIMENTAL DATA
THEORETICAL CURVE OF SLOPE - 1/2
10^2
10^3
10^4
FREQUENCY, CYCLES PER SECOND

hundred seconds. Desicote, a Beckman product which forms a hydrophobic surface layer when applied to clean air-dry glass, was forced through the capillary and the tube was air-dried by forcing clean filtered air through it for several hours. When the electrode assembly of Figure 1 was replaced by this capillary, at the end of which mercury droplets could form and act as an electrode, and a platinized platinum gauze which served as a reference electrode, measurements of capacity and resistance could be made with a precision approaching that achieved with the flat surfaces.

The procedure for measurement involved setting a capacity value on the variable arm of the bridge and observing the variation of the Lissajou figure depicting the state of bridge balance passes through a horizontal straight line configuration. At this instant, the size of the droplet is such that its double layer capacity and its resistance are just the proper values to balance the bridge. By finding flow rate as a function of time and assuming a spherical shape for the mercury droplet at the instant of balance, the age of the drop can be used as a measure of the surface area. Measurements of capacity, resistance, and associated drop age were made at fixed polarizations for several frequencies. Rather than convert to capacity per unit area using the assumptions just mentioned, the data are displayed in graphical form. Measured capacity vs. time on a log-log plot in Figure 24 shows

Figure 24. Capacity of an expanding surface of a mercury droplet as a function of growth time. Mercury extruded from a Desicote treated capillary

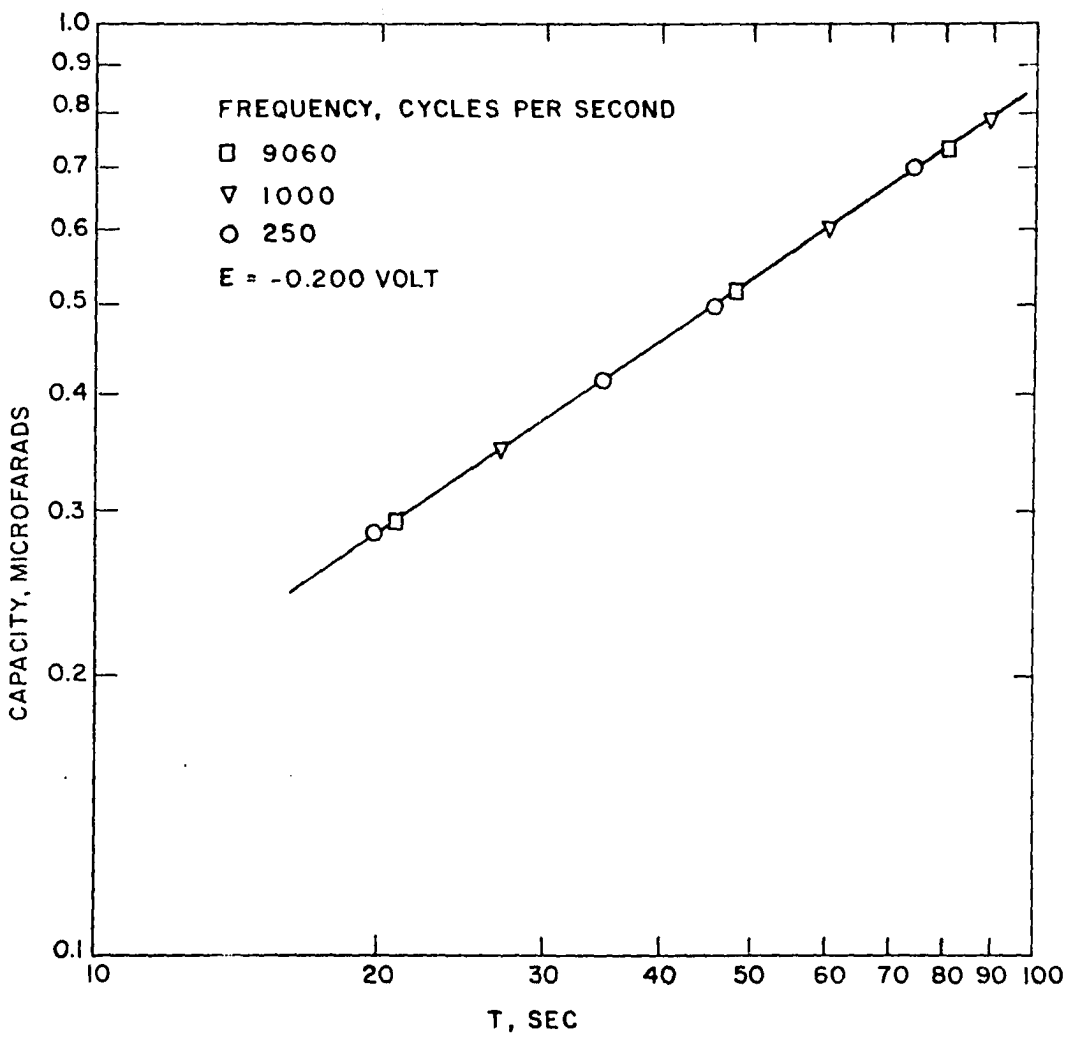
FREQUENCY, CYCLES PER SECOND
□ 9060
▽ 1000
○ 250
E = -0.200 VOLT
CAPACITY, MICROFARADS
1.0
0.9
0.8
0.7
0.6
0.5
0.4
0.3
0.2
0.1
10
20
30
40
50
60
70
80
90
100
T, SEC

that values for all frequencies lie on the same straight line with several times for identical frequencies serving to establish the linear character of the log capacity vs. log time relationship. Resistance values are similarly displayed in Figure 25 and show the same linear character of log resistance vs. log time. The slopes of the log-log plots should be 2/3 for the capacity-time curve in Figure 24 and -1/3 for the resistance-time curve in Figure 25 if a constant volume flow rate exists and if the drops are spherical. These slopes follow from

$$V = \frac{4}{3}\pi r^3 \quad \text{for the volume of a sphere} \tag{46}$$

and

$$V = kt \quad \text{for the volume delivered in time, t, when k is a constant flow rate.} \tag{47}$$

When the time variable is considered zero at the beginning of the drop then Equation 47 gives the volume of a drop as a function of its age. Then from Equations 46 and 47

$$r^3 = \frac{3k}{4\pi} t \tag{48}$$

and

$$r^2 = \left(\frac{3k}{4\pi}\right)^{\frac{2}{3}} t^{\frac{2}{3}}. \tag{49}$$

Since the surface area of a sphere is given by

$$S = 4\pi r^2 \tag{50}$$

and the double layer capacity at a surface by

$$C = C_o S \tag{51}$$

Figure 25. Resistance as a function of growth time for a growing mercury droplet. Mercury extruded from a Desicote treated capillary

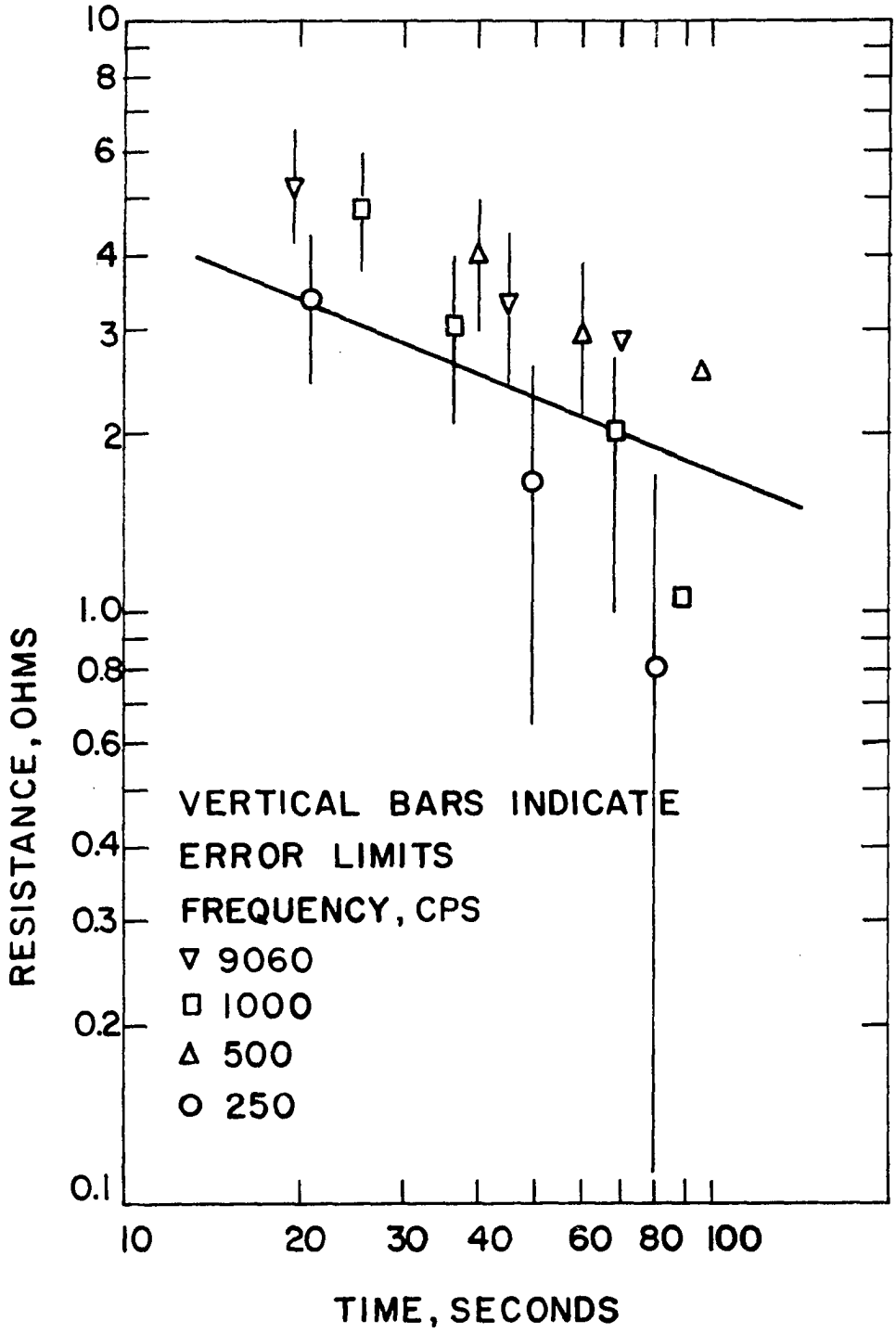
10
8
6
4
3
2
1.0
0.8
0.6
0.4
0.3
0.2
0.1
RESISTANCE, OHMS
VERTICAL BARS INDICATE
ERROR LIMITS
FREQUENCY, CPS
▽ 9060
□ 1000
△ 500
○ 250
10
20
30
40
60
80
100
TIME, SECONDS

then

$$C = 4\pi C_o \left(\frac{3k}{4\pi}\right)^{\frac{2}{3}} t^{\frac{2}{3}}.$$

A few values of capacity per unit area were calculated and agreed well with Grahame's results (10). On the other hand, the resistance between two concentric spheres of radii r_1 and r_2 (32, 33) is given by

$$R = \left(\frac{1}{r_1} - \frac{1}{r_2}\right) \frac{\sigma}{4\pi} \tag{52}$$

where σ is the resistivity of the medium between the spheres. If r_2 becomes large compared to r_1, the approximation

$$R = \frac{\sigma}{4\pi r_1} \tag{53}$$

applies and can be used if a large cylinder replaces the large sphere. From Equation 48 we have

$$r = \left(\frac{3k}{4\pi}\right)^{\frac{1}{3}} t^{\frac{1}{3}} \tag{54}$$

which, with Equation 53, gives

$$R = \frac{\sigma}{4\pi}\left(\frac{4\pi}{3k}\right)^{\frac{1}{3}} t^{-\frac{1}{3}}. \tag{55}$$

It is obvious that the measured values of R and C also had to be corrected by the calibration procedure previously outlined and that the corrected values of R had to be further adjusted to take into account the rather large resistance of the mercury column in the precision bore capillary.

Finally, we present data to demonstrate that a dispersion

in resistance and capacity occurs when measurements are made on droplets extruded from a capillary which has not been treated with Desicote. A distinct curve of capacity vs. time is obtained for each frequency in Figure 26. Similarly variation of resistance with frequency is shown in Figure 27.

Thus, we have two cases exhibiting dispersion in the apparent double layer capacity for which plausible arguments can be made in support of the existence of spurious thin films of solution in the electrode mounting assembly. In a rough quantitative fashion, the dispersion can be explained in terms of properties of the film, for one case at least. On the other hand, dispersions in capacity and in resistance were not evident in a case for which electrode preparation was of such a nature as to prevent the formation of a spurious thin film of solution in the support assembly. We conclude, therefore, that dispersions in capacity and resistance measured as functions of frequency in the absence of surface active substances are not reflections of properties of the electrical double layer but are due to improper electrode design.

Figure 26. Capacity of growing mercury drop at intervals during its expansion. Droplets extruded from untreated capillary

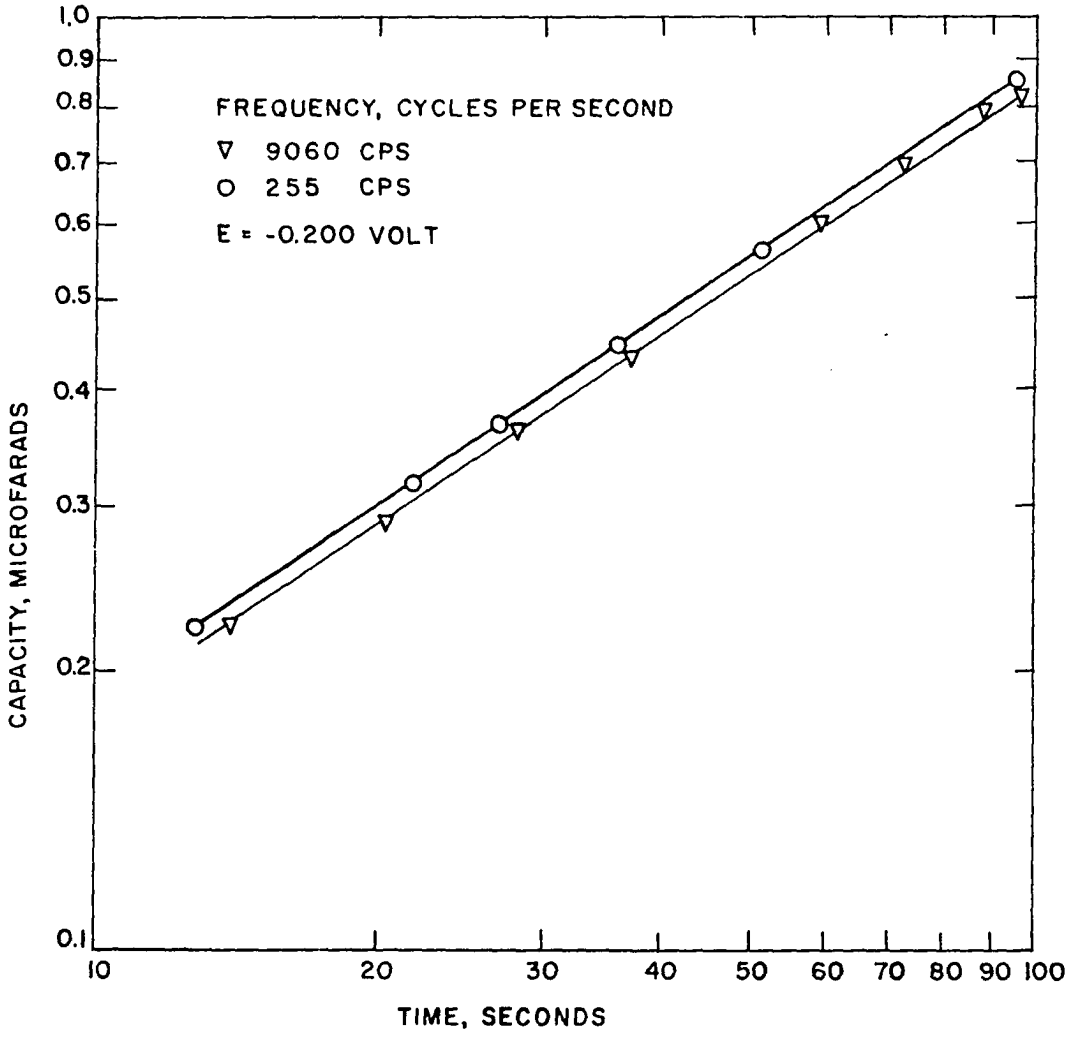
FREQUENCY, CYCLES PER SECOND
▽ 9060 CPS
O 255 CPS
E = -0.200 VOLT
CAPACITY, MICROFARADS
1.0
0.9
0.8
0.7
0.6
0.5
0.4
0.3
0.2
0.1
10
20
30
40
50
60
70
80
90
100
TIME, SECONDS

Figure 27. Resistance for growing mercury drop at intervals during life. Droplets extruded from untreated capillary

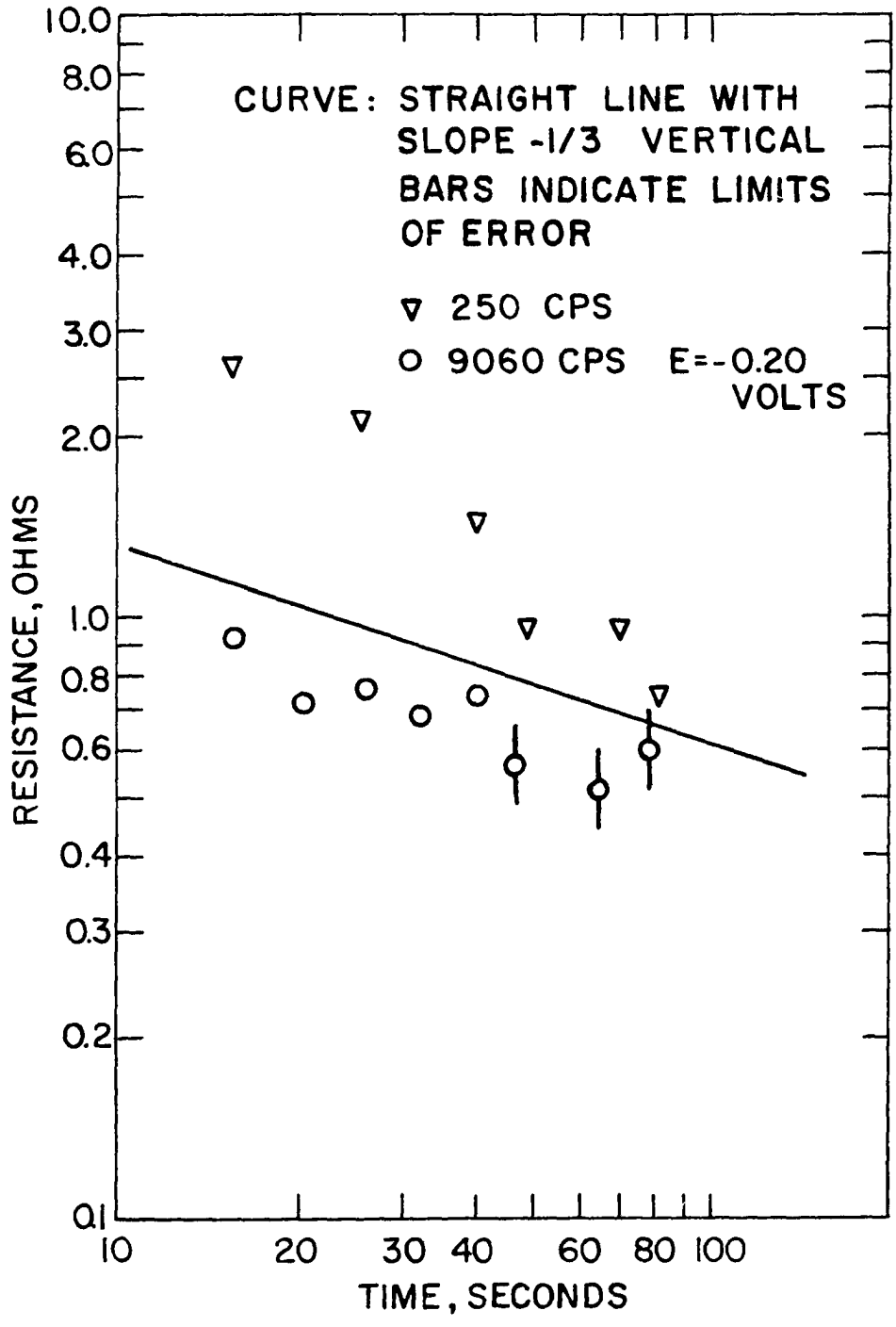
CURVE: STRAIGHT LINE WITH SLOPE -1/3 VERTICAL BARS INDICATE LIMITS OF ERROR
▽ 250 CPS
○ 9060 CPS E=-0.20 VOLTS
RESISTANCE, OHMS
10.0
8.0
6.0
4.0
3.0
2.0
1.0
0.8
0.6
0.4
0.3
0.2
0.1
10
20
30
40
60
80
100
TIME, SECONDS

SUMMARY

After assembling an instrument capable of high sensitivity, a substitution technique was applied to investigate the frequency dependence of the double layer capacitance at the interface between mercury and aqueous electrolytic solutions for several polarizations of the mercury and for three temperatures. Several electrode designs for forming the interface were tested for reproducibility of the measurements with particular emphasis placed on those designs permitting a flat interface to be formed.

It was shown that the frequency dependences of both the capacitance and resistance was due to a distributed capacity effect analogous to that which is found in the transmission lines of communications engineering. An annulus was postulated to exist between the supporting glass sheath and the gold tube at the end of which the flat mercury interface was formed. A reasonable value for the separation of gold and glass was assumed and proved to be sufficient to account for the observed trend and order of magnitude of the frequency dependence of the capacitance and resistance.

A complete frequency independence of the capacity and resistance was demonstrated for an interface between a mercury droplet and electrolytic solution. The droplet was extruded from a capillary of about 65 microns internal diameter having

a hydrophobic inner wall. Application of Desicote to the inner wall was sufficient to prevent solution penetration between the glass of the capillary and the mercury thread and thus remove the source of the distributed capacity effect. This effect had not been eliminated by others using the growing mercury drop who reported small capacity variations with frequency and large but not reproducible resistance variations variously attributed to shielding of the droplet and to a relaxation process in the double layer.

CONCLUSIONS AND RECOMMENDATIONS

Doubtless the most important result of this investigation is the demonstration of a complete absence of a frequency effect in measurements of double layer capacity and associated cell resistance in the audio frequency range. This is in agreement with the findings of Frumkin (8) who measured capacity up to the megacycle range but did not report on resistance while it contradicts Bockris's (21) reported resistance variations for mercury and both resistance and capacitance variations for copper electrodes up to about 2000 cycles per second. Any relaxation process which can be stimulated by an alternating electric field must therefore have a half life outside the range 10^{-8} second to 5×10^{-2} second, for the measurements of Frumkin should have detected effects as fast as the lower time limit while the audio measurements of this work should have found the slower effects.

A second point to be made is that extreme care must be used in the design of experiments to examine kinetic effects in electrode processes, whether one is concerned with a non-polarizable or a polarizable electrode. The width of the annulus between metal and glass support of the electrode used in this research was estimated to be of the order of 3 microns. In the absence of evidence to the contrary, intuition would regard this as so small that its contribution to the admittance

of the electrode could be neglected. The calculations shown in the discussion section demonstrate the contrary. Further, one can compare the results of measurements obtained at mercury droplets extruded from capillaries with hydrophobic inner walls with measurements on drops formed at the ends of capillaries with untreated inner walls. Solution penetration in the latter case must result in a very thin liquid film between mercury and glass and an attendant high resistance in the film. Yet resistance variations are appreciable.

The use of a flat static interface for measurements of the capacity is very attractive despite the difficulties demonstrated in this research. It seems reasonable that electrodes utilizing an outer case of a resin rather than glass could be made. The gold tube which was mounted by sealing in glass could be supported in a mold filled with an epoxy resin which could be polymerized at room temperature. No annulus should appear between the gold and supporting epoxy resin if the temperature does not vary greatly from the polymerization temperature. Formulations of epoxy resins are available commercially which require only that one mix two components in proper proportions and allow to harden. Hardening occurs in a matter of hours. Ciba Products Corporation markets one such product under the trade name Araldite. Choice of a resin should be carefully made to avoid a low molecular weight resin with slightly soluble surface active components in the poly-

merized product. The remainder of the electrode preparation could be identical to that used for the glass mounted one.

If dynamic measurements on growing mercury droplets are necessary or desirable, polytetrafluoroethylene or polymonochlorotrifluoroethylene could be used to make capillaries with hydrophobic properties from which mercury could be allowed to flow. These polymers are available commercially as Teflon and Kel-F, respectively. Fabrication of capillaries from these materials would doubtless be easier than applying Desicote or cetyl pyridinium bromide to the interior walls of capillaries 50 to 75 microns in radius.

BIBLIOGRAPHY

1. Quincke, G. Annalen der Physik und Chemie. Series 2. [Pogg. Ann.]. 113: 513. 1861.

2. Matsuda, H. J. Physical Chemistry. 64: 336. 1960.

3. Hansen, R. S., Hickson, D. A., and Mintern, R. E. J. Physical Chemistry. 61: 953. 1957.

4. Grahame, D. C. J. Chemical Physics. 23: 1166. 1955.

5. Green, M. J. Chemical Physics. 31: 200. 1959.

6. Gibbs, J. W. The collected works of J. Willard Gibbs. 2nd ed. Vol. 1. New Haven, Conn., Yale University Press. 1928.

7. Lippmann, M. G. J. de Physique et le Radium. Series 2. [J. de Physique Theoretique et Appliquée]. 2: 116. 1883.

8. Frumkin, A. and Proskurnin, M. Transactions of the Faraday Society. 31: 110. 1935.

9. Grahame, D. C. J. American Chemical Society. 71: 2975. 1949.

10. _____. Chemical Reviews. 41: 441. 1947.

11. Lippmann, M. G. Annales de Chimie de Physique. Series 5. 5: 494. 1875.

12. Craxford, S. R. Electrocapillary phenomena. Photocopy. Unpublished Ph. D. dissertation. Oxford, England, Bodleian Library, Oxford University. 1936.

13. Debye, P. Handbuch der Radiologie. 6: 597. 1925.

14. Grahame, D. C. J. Chemical Physics. 18: 903. 1950.

15. Ershler, B. V. Zhurnal Fizicheskoi Khimii. Series 7, 20: 679. 1946. Original available but not translated; translation in R. W. Hummel. The discrete structure of charge in a double layer. U.S. Atomic Energy Commission Report NP-tr 869. [Technical Information Service Extension, AEC]. 1962.

16. MacDonald, J. R. J. Chemical Physics. 22: 1857. 1954.

17. Watts-Tobin, R. J. Philosophical Magazine. 6: 133. 1961.

18. Loveland, J. W. and Elving, P. J. Chemical Reviews. 51: 67. 1952.

19. Grahame, D. C. J. American Chemical Society. 68: 301. 1946.

20. Frumkin, A. and Melik-Gaikazyan, V. I. Doklady Akademiia Nauk S. S. S. R. 77: 855. 1951. Determination of the kinetics of adsorption of organic substances by measurement of the differential capacity and the conductance of the boundary between electrodes and solution. (Translated title) Original available but not translated; translation available from Amherst, Mass., Department of Chemistry, Amherst College.

21. Bockris, J. O'M. and Conway, B. E. J. Chemical Physics. 28: 707. 1958.

22. Grantham, D. H. Electrical double-layer impedance at the mercury-aqueous perchloric acid interface. Unpublished M. S. thesis. Ames, Iowa, Library, Iowa State University of Science and Technology. 1959.

23. Gordon, D. L. and Wichers, E. Annals of the New York Academy of Science. 65: 369. 1957.

24. Jones, G. and Bullinger, G. M. J. American Chemical Society. 53: 411. 1931.

25. Debye, P. Polar molecules. New York, N. Y., Chemical Catalog Co. 1929.

26. Fröhlich, H. Theory of dielectrics. Oxford, England, Clarendon Press. 1949.

27. Smythe, C. P. Dielectric behavior and structure. New York, N. Y., McGraw-Hill Book Co., Inc. 1955.

28. Kurosaki, S. J. Physical Chemistry. 58: 320. 1954.

29. Zimmerman, J. R., Holmes, B. G., and Lasater, J. A. J. Physical Chemistry. 60: 1157. 1956.

30. Hansen, R. S. and Hickson, D. A. Adsorption kinetics from double layer capacitance measurements. [Mimeographed Paper 23]. In Symposium on Charge Transfer Processes, Toronto, Canada, Sept. 4-5, 1958. Ottawa, Canada, Chemical Institute of Canada, Physical Chemistry Division. 1958.

31. Handbook of chemistry and physics. 36th ed. Cleveland, Ohio, Chemical Rubber Publishing Co. 1954.

32. Ryder, J. O. Networks, lines, and fields. New York, N. Y., Prentice-Hall, Inc. 1949.

33. Rogers, F. E. The theory of networks in electrical communication and other fields. London, England, MacDonald and Co., Ltd. 1957.

34. Coulson, C. A. Electricity. New York, N. Y., Interscience Publishers, Inc. 1958.

35. Smythe, C. P. Static and dynamic electricity. 1st ed. New York, N. Y., McGraw-Hill Book Co. 1939.

ACKNOWLEDGMENT

Thanks are due Professor R. S. Hansen for his encouragement and enthusiasm without which this work would not have been completed.